ADVANCED TECHNOLOGY FOR RAILWAY HYDRAULIC HAZARD FORECASTING

A Thesis

by

WILLIAM EDWARD HUFF

Submitted to the Office of Graduate Studies of
Texas A&M University
in partial fulfillment of the requirements for the degree of

MASTER OF SCIENCE

Approved by:

Co-Chairs of Committee,	Kelly Brumbelow
	Tony Cahill
Committee Member,	Brad Wilcox
Head of Department,	John Niedzwecki

December 2012

Major Subject: Civil Engineering

ABSTRACT

Railroad bridges and culverts in the United States are often subject to extreme floods, which have been known to washout sections of track and ultimately lead to derailments. The potential for these events is particularly high in the western U.S. due to the lack of data, inadequate radar coverage, and the high spatial and temporal variability of storm events and terrain.

In this work, a hydrologic model is developed that is capable of effectively describing the rainfall-runoff relationship of extreme thunderstorms in arid and semi-arid regions. The model was calibrated and validated using data from ten storms at the semi-arid Walnut Gulch Experimental Watershed. A methodology is also proposed for reducing the amount of raingages required to provide acceptable inputs to the hydrologic model, and also determining the most appropriate placement location for these gages.

Results show that the model is capable of reproducing peak discharges, peak timings, and total volumes to within 22.1%, 12 min, and 32.8%, respectively. Results of the gage reduction procedure show that a decrease in the amount of raingages used to drive the model results in a disproportionally smaller decrease in model accuracy. Results also indicate that choosing gages using the minimization of correlation approach that is described herein will lead to an increase in model accuracy as opposed to selecting gages on a random basis.

ACKNOWLEDGEMENTS

First, I would like thank my graduate advisors, Dr. Kelly Brumbelow and Dr. Tony Cahill, for their constant guidance and assistance in this project, without which this would not be possible. I have learned a great deal from these men over the past two years and I am very grateful.

I am also very thankful for my wonderful friends and family. Thank you all for your love and support throughout my education.

I would also like to acknowledge the USDA-ARS Southwest Watershed Research Center for providing most of the data used in this project, I would specifically like to thank Dr. David Goodrich for his assistance in locating some of this data.

Finally, I would like to express my gratitude to the Association of American Railroads (AAR) who funded this project. I hope that what has been learned can be a benefit to the railroads and make them safer.

TABLE OF CONTENTS

Page

LIST OF FIGURES

LIST OF TABLES

1. INTRODUCTION*

1.1 Problem Statement

Trains provide an efficient method of transportation for people and goods across the United States, and are essential for commerce and keeping the economy on track (Blanton and Marcus, 2009). In creating the extensive network of railroad infrastructure required for this trade to be possible, these railroads have no choice but to cross numerous drainage networks and are consequently subject to damages from flooding. Railroads are particularly susceptible to impairment from flash floods, or extreme hydrologic events that have a relatively rapid time-to-peak. If a crossing is not of adequate size to accommodate the large flood discharge, scouring can occur and undermine the track subgrade, or even wash out the crossing completely. These washouts or "railway hydraulic hazards" have been known to occur anywhere from large bridge crossings to small culvert crossings. As these events occur very quickly, there is often little time for identification of these track failures, and many ultimately lead to derailments as trains attempt to cross these washed out sections of track without knowing of the threat that lies ahead.

Over the past thirty years in the U.S., railway hydraulic hazard events have resulted in over $105 million in railroad track and equipment damages, as well as several casualties (Huff, et al. 2012).

---

*Reprinted with "Advanced Technology for Railway Hydraulic Hazard Forecasting by Huff, W. E., Brumbelow, J. K., and Cahill, T. C., 2012. *World Environmental and Water Resources Congress 2012: Crossing Boundaries, ASCE,* Albuquerque, NM, May 20-24, 2012. Copyright 2012 by ASCE.

Table 1.1 shows the damages resulting from these events as reported to the Federal Railroad Administration (FRA) for the period of 1982-2011. This data was compiled from the FRA Office of Safety Analysis website (FRA, 2011). A map of the railway hydraulic hazard events over the same time period is displayed in Figure 1.1.

Table 1.1. U.S. Railway Hydraulic Hazard Damage Statistics

Railway Hydraulic Hazard Events (1982-2011)	
Incidents:	263
Equipment/Track Damages:*	$105,741,067
Fatalities:	14
Injuries:	211
Average Damages Per Incident:*	$402,057
Maximum Single Event Damages:*	$6,200,500

*Does not include value of lost revenue or loss of life

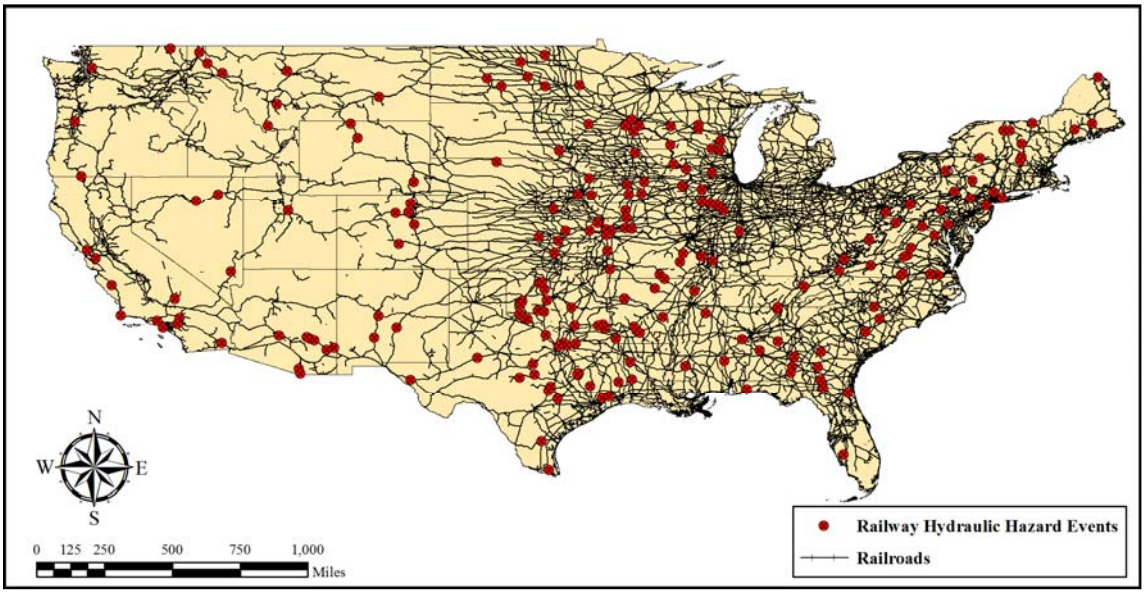

Fig. 1.1. Map of Total Railway Hydraulic Hazard Events from 1982-2011

1.2 Project Scope

The scope of this project is the remote western United States, which is dominated by arid and semi-arid climates. This location was selected for the project due to its increased potential for flash flooding, as well as the unique challenges that exist to modeling in the region.

While there are many factors that are taken into consideration, the primary metric used to define aridity is the average annual precipitation of an area. Arid and semi-arid regions can be classified as those in which the average annual precipitation falls between 50-200 mm/yr and 200-500 mm/yr (approximately 2-8 in./yr and 8-20 in./yr), respectively (Lloyd, 1986). There are many factors that make arid and semi-arid regions especially prone to flash flooding events. Although these areas are characterized by a relatively dry environment and low annual rainfall, storm events in arid and semi-arid regions are often high in intensity and have a high spatial and temporal variability. Most of these flash flood-producing storms are convective thunderstorms, generally occurring in the summer months. These storms are generated by moist air which combines with strong convective heating, made possible by the lack of cloud cover and the dry surface conditions typical of the region (Osborn et al. 1970). As the precipitation rate resulting from these storms typically exceeds the infiltration capacity of the soil, runoff production is consequently controlled by the Hortonian, or infiltration excess, mechanism (Horton, 1933).

Arid and semi-arid regions are also predominately characterized by large areas of bare soils, usually having a low permeability. These poorly-drained soils, when

combined with high intensity storms, usually result in an enormous amount of runoff and ultimately an elevated potential for flash flooding. McIntyre (1958) attributes the low permeability of arid soils to the formation of a thin compacted crust layer on the surface of bare soils, which has a sealing effect on the surface. Adding to the already high flash flood potential, the high temperatures and overall lack of moisture make arid and semi-arid regions more prone to wildfires. As Neary et al. (2005) points out, wildfires can increase runoff by removing surface vegetation and making soils "hydrophobic", or water repelling, decreasing their infiltration capacity.

One problem typical of the western U.S. that makes it particularly difficult to model is the overall lack of observed data. Many of the more remote areas are severely lacking in real-time rainfall and stream-flow monitoring stations, as well as competent rainfall-runoff models to predict the resulting floods, and also past data from which to calibrate these models. This often necessitates the use of overly complex models that can be extremely data and time intensive.

Yet another problem that characterizes the western U.S. is the limited weather radar coverage. The National Weather Service has around 148 Next Generation Radar (NEXRAD) stations which are capable of sensing most precipitation within approximately 90 mi of the radar, as well as intense rain or snow within approximately 155 mi of the radar stations (Weather Underground, 2011). As highlighted by Figure 1.2, several of these NEXRAD stations in the western U.S. are spaced farther than this effective 90 mi coverage distance, leaving these areas potentially blind to approaching storms and increasing the potential for railway hydraulic hazard events. In 2002, the

National Weather Service Western Region (NWS-WR) identified a list of features that a flash flood forecasting model should include (Gupta et al., 2006). One of the major requirements identified was the inclusion of a rainfall-runoff model that was capable of using radar precipitation inputs. This is clearly not possible in areas where there is limited radar coverage, making the use of other precipitation inputs essential.

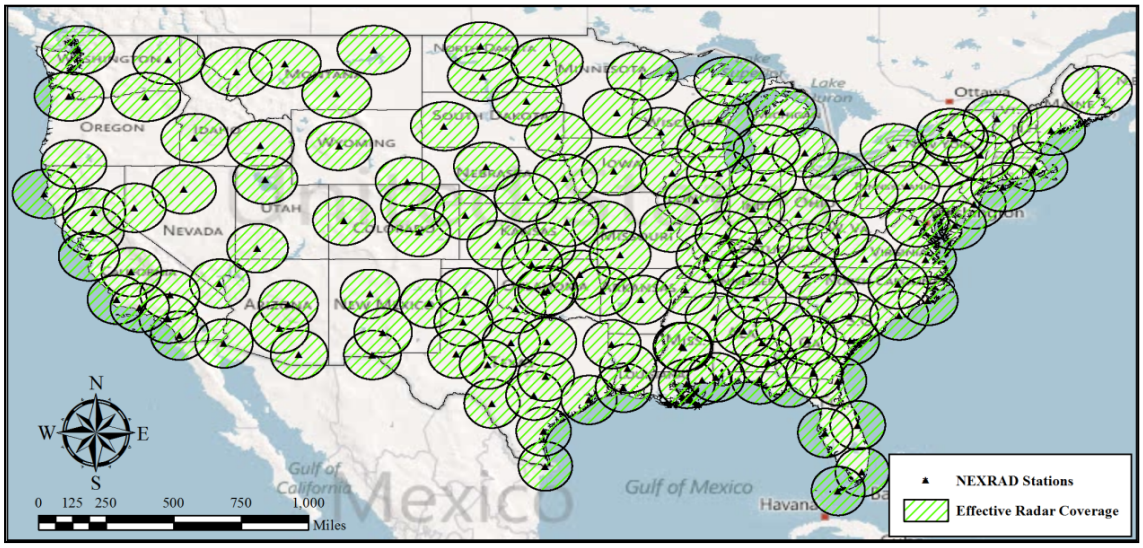

Fig. 1.2. 90 mi Effective Radar Coverage for Reliable Rainfall Rate Determination

To summarize, railroads in the arid and semi-arid western United States are highly susceptible to hydraulic hazard related derailments, which can be attributed to numerous problems including:

- An elevated potential for flash flooding in the region,
- Lack of real-time and historical rainfall and stream-flow data,

- High intensity thunderstorms that are extremely variable in space and time, and
- Limited weather radar coverage in the region.

1.3 The Railway Hydraulic Hazard Monitoring System

Through an ongoing project with Texas A&M University and the Association of American Railroads (AAR), researchers have investigated the feasibility of a web-based decision support system, the Railway Hydraulic Hazard Monitoring System (RHHMS), for real-time forecasting of potential railway hydraulic hazard events (Peschel, et al. 2010). The goal of RHHMS is to convey information from a complex series of dynamic hydrologic calculations, into a simple visualization of flood hazards for railway bridges that have been identified as particularly vulnerable.

To facilitate RHHMS, researchers have also investigated the use of an economic package of raingages, soil moisture sensors, and stream gages, to provide data to a hydrologic model for advanced identification of these flash flood events. In the final phase of this project, these real-time sensors would ultimately provide precipitation and soil moisture data to the model through a telemetry system. In addition, a real-time web camera would potentially be positioned at each instrumented crossing to provide further confirmation of a potential threat to the railway structure. The objective of this proposed combinatorial optimization approach to hydrologic measurement is to provide multiple lines of evidence, for greater accuracy, as well as redundancy in the event that one or more of the instruments malfunction.

For each of the instrumented sites, this approach would allow for both the current and the forecasted flow conditions at the crossing to be displayed and an alert could then be issued to railroad operators if a structure is in danger of sustaining damage. Railroad officials have also expressed interest in a wayside system tied directly into a signal alongside the track. This feature would take the decision-making out of the hands of railroad operators and ultimately lead to a quicker response. While a prototype of the RHHMS user interface has been developed in previous work, RHHMS is still far from operational.

1.4 Motivation and Objective of Study

The primary goal of this thesis is to identify and develop a hydrologic model that can be used to provide adequate flood forecasts to RHHMS. The model must be capable of accurately predicting the rainfall-runoff relationship of extreme storm events in remote arid and semi-arid basins. Requirements of the model include being able to operate in areas where the radar coverage is limited (i.e. operate using raingage data), being able to account for the spatial and temporal variability of storm events as well as parameter data, and being able to operate with relatively small time steps in order to accurately model flash flood events.

Once a suitable hydrologic model has been identified, the model must be calibrated and validated using gaged data from an arid or semi-arid watershed in the western U.S. Specifically; the objective of this process is to minimize the modeled error

in peak discharge. Secondary objectives include minimizing the modeled error in peak timing and total runoff volume.

Another major goal of this work is to identify a methodology for reducing the number of raingages that are used to provide inputs to a hydrologic model, while still maintaining an acceptable level of model prediction accuracy. The specific objectives of this methodology include minimizing the costs associated with hydrologic measurement as well as maximizing the capacity of a gage network to accurately capture the spatial variability of rainfall in a particular area. By reducing the density of a gage network and examining the changes in model performance, this can provide some insight into the tradeoff between the density of a raingage network, versus the resulting prediction accuracy of the hydrologic model that it provides inputs to.

In summary, the specific goals of this project include the following:

- Develop a hydrologic model capable of effectively predicting the runoff peak discharge and timing resulting from high intensity, spatially variable storm events in arid and semi-arid areas,
- Calibrate and validate the model using data from a semi-arid watershed in the western U.S., and
- Determine a methodology for reducing the number of raingages that are used to provide inputs to the model, while still providing an acceptable level of model accuracy.

2. LITERATURE REVIEW

2.1 Introduction to Rainfall-runoff Modeling

One of the primary tools of the hydrologist is the rainfall-runoff model, also known as the hydrologic or watershed model. A rainfall-runoff model is a mathematical tool used to simulate hydrologic processes, in which the major input is precipitation and the major output is the runoff hydrograph, describing the volume and timing of flood discharges. Some models are simpler, in that they only calculate the peak discharge volume instead of the complete hydrograph. The system in which this occurs is the watershed, also known as the catchment or basin. The hydrologic processes in the model that are used to convert rainfall to runoff typically include evapotranspiration, interception, detention storage, soil moisture accounting, infiltration, overland flow, channelized flow, and groundwater flow. To date, there are hundreds of these models being used in a variety of different applications. Models are selected based on the environment in which they will be used as well as the existence of data, as well as the quality of data that are available, and are typically classified to help convey their suitability for a particular application. Each model has its own unique strengths and weaknesses depending on the situation in which it is used. While there is no universal classification system for rainfall-runoff models, three categories will be discussed herein, including empirical and conceptual models, lumped and distributed-parameter models, as well as event-based and continuous simulation models.

Rainfall-runoff models can be described as either empirical or conceptual (Wurbs and James, 2002). Empirical models rely on historic gaged data and attempt to reproduce observed flows using best-fit equations. These models contain minimal or no physical transfer functions to relate the input to the output, but rather rely on finding a statistical relationship between the two (Anderson and Burt, 1985). Empirical models are generally developed for specific locations and situations, and can be very useful if adequate data exists for the study area. One popular example of an empirical model is the unit hydrograph method (Sherman, 1932). Conceptual models, also known as physically-based models, are derived from physical equations including conservation of mass, momentum, and energy, and attempt to simulate the actual physical processes involved in runoff production and routing. As conceptual models usually require less gaged data to calibrate, they are more easily applied to ungaged basins. While these models are powerful, they also come with a price in that they are very data and time intensive, but they are becoming much more feasible with the increasing availability of digital data. Examples of conceptual models include KINEROS (Woolhiser et al., 1990) and GSSHA (Downer and Ogden, 2006).

Rainfall-runoff models can also be classified as either lumped-parameter or distributed-parameter models. Lumped-parameter models spatially average the parameters of a watershed (i.e. surface roughness coefficient, soil saturated hydraulic conductivity, etc.) over the entire area and treat the watershed as a single unit. Widely used examples of lumped-parameter models include the Rational Method (Kuichling, 1889) and the Curve Number method (NRCS, 1986). Distributed-parameter models

subdivide a watershed into smaller elements or grid cells, and attempt to account for the spatial variability of parameters by simulating the hydrologic processes that take place within each element. It should be noted, however, that all models are lumped to a certain degree, and are limited by the resolution of the parameter data that is available. KINEROS and GSSHA are also example of distributed models.

Finally, models can be described as being either event-based or continuous simulation. Event-based, also known as event-oriented, models are used to simulate individual storm events over relatively short periods of time. The time scales used for event-based models are generally small, and typically range from minutes to hours (Knapp et al. 1991). Event-based models usually do not include processes that account for changes in soil moisture. Continuous simulation models are generally used to simulate longer periods of time and can include multiple precipitation events as well as the dry periods in between. Evapotranspiration and soil moisture accounting are usually incorporated in continuous simulation models in order to maintain a water balance in between storms. These models typically have a larger time scale, usually ranging from less than an hour to several days (Knapp et al. 1991).

2.2 Physically-based, Distributed-parameter Models

The Kinematic Runoff and Erosion model (KINEROS) is an example of a physically-based, distributed-parameter, event-based model that was developed by Woolhiser et al. (1990) to estimate the hydrologic response of ungaged watersheds. In this model, watersheds are broken up into a cascade of one-dimensional overland flow

and channel elements, and routed downstream using an approximation of the kinematic wave equation (Woolhiser et al., 1990). The model uses Hortonian infiltration-excess, generated overland flow processes to calculate the amount of surface runoff that is produced.

Like the KINEROS model, CASC2D is also a physically-based, distributed parameter model that was developed by Julien et al. (1995) and funded by the U.S. Army and the Environmental Protection Agency (EPA) to simulate runoff generated by the Hortonian mechanism. The major processes simulated by the CASC2D model include rainfall distribution, interception, infiltration, two-dimensional overland flow routing, and one-dimensional channelized flow routing. While the two models are very similar, the primary difference between KINEROS and CASC2D is that CASC2D uses an approximation of the diffusive wave equation to route flow, instead of the kinematic wave equation that is used in the KINEROS model. Also, CASC2D is capable of continuous simulations as well as single event simulations. Among the objectives in the formulation of CASC2D was the need to accurately simulate flash floods caused by intense thunderstorms. The model has been proven to work well in remote arid and semi-arid regions, where the principal runoff production mechanism is generally Hortonian (Downer, et al. 2002). Senarath et al. (2000) used the Goodwin Creek Experimental Watershed in northeast Mississippi to test and verify the capabilities of the CASC2D model. Researchers concluded that the model was successful in reproducing flows at the outlet as well as interior stream gages. Ogden et al. (2000) used CASC2D to successfully simulate the extreme flooding that occurred in Fort Collins, Colorado in 1997, which

caused significant damage to the city including railroad infrastructure and ultimately led to a train derailment.

2.3 Real-time Hydrology and Flash Flood Forecasting

Flash floods are defined as those occurring less than 6 hours of the causative storm event (NWS, 2002). These floods account for the highest amount of casualties among all natural disasters, and billions of dollars in property damages each year (AMS, 1985). The National Weather Service (NWS) provides flood warnings to the U.S., and is divided into 13 River Forecast Centers (RFC's). These RFC's provide daily river forecasts using two rainfall-runoff models (Gupta and Schaffner, 2006). The two models that are used in these predictions are the Sacramento Soil Moisture Accounting Model (SAC-SMA), and the Continuous-API Model (CONT-API), which is based on the Antecedent Precipitation Index (API; Kohler and Linsley, 1951). SAC-SMA is a continuous, lumped parameter model which is conceptual in nature (Burnash et al., 1973). CONT-API is also a continuous, lumped-parameter model, however is empirical in nature (Sittner et al., 1969). Both of these models run at either a 6-hour or a 1-hour time step, which can be inadequate for a short-fused flash flood event.

Flash flood warnings are issued on a county-by-county basis using rainfall-runoff models similar to those of the RFC's, but which run at either a 1-hour or 0.5-hour time step (Yatheendradas, 2007). Model inputs come from areal average rainfall values calculated using a combination of radar and gage data. While these models can be very effective in some regions, they are not very accurate for arid and semi-arid regions as the

models are lumped, and cannot accurately convey the spatial heterogeneity of either the rainfall or the watershed parameters. Furthermore, the time steps used in the models are too large to simulate flash floods, which can peak in less than 15 minutes in some cases (Yatheendradas, 2007).

Gupta and Schaffner (2006) recommend that a good flash flood forecasting model should include the following:

- Account for rainfall inputs with a high spatial and temporal variability,
- Be distributed-parameter to account for spatial heterogeneities,
- Include an infiltration-excess runoff mechanism, and
- Be able to accurately represent channel transmission losses.

Yatheendradas et al. (2008) suggests that protection from flash flooding can be best achieved by implementing a real-time warning system with a built in hydrologic model. Researchers used the KINEROS2 model along with data from storm events at the Walnut Gulch Experimental Watershed to evaluate sources of uncertainty in such a system. Researchers found that uncertainties existing in rainfall estimates, model parameters and initial conditions are very significant, and can greatly reduce the reliability of a flash flood forecasting model (Yatheendradas et al. 2008).

2.4 Walnut Gulch Experimental Watershed

The hydrologic model developed for RHHMS was tested and validated using ground based hydrologic data from the Walnut Gulch Experimental Watershed (WGEW) located in southeastern Arizona. In 1953, research was initiated at WGEW by

the Research Division of the Soil Conservation Service (SCS) for the purpose of improving the knowledge of hydrologic processes in semi-arid rangelands. Currently, the site is touted as the foremost semi-arid experimental watershed in the world (USDA, 2003) and is operated by the USDA Southwest Watershed Research Center (SWRC). The watershed encompasses approximately 149 km² of land in the upper San Pedro River Basin and is dominated by desert shrubs in the lower two-thirds and grasses in the upper one-third (Renard et al., 2008). Streams in the WGEW are ephemeral and are dry for the majority of the year, and almost all of the runoff events are generated by high-intensity convective thunderstorms during the summer months (USDA, 2003). At WGEW, the interaction of groundwater flow does not play a significant role in runoff production as the groundwater table lies from 50 m to 145 m below the land surface. Instrumentation at the site includes 88 raingages and 11 flumes, all outfitted with electronic sensors and data loggers that collect data and transmit it by means of radio telemetry to a computer at the SWRC office in Tombstone where the data is archived.

3. MODELING APPROACH

3.1 Model Description and Overview

While the RHHMS hydrologic model was developed and coded independently, it is based largely upon the principles of the U.S. Army Corps of Engineers' Gridded Surface/Subsurface Hydrologic Analysis (GSSHA) model (http://chl.erdc.usace.army.mil/gssha). The GSSHA model is an evolution of CASC2D, and was developed by Ogden et al. (2000) to extend the modeling capabilities of CASC2D to non-Hortonian watersheds, and include the interaction of groundwater flow when saturation excess is the primary runoff production mechanism. Unlike its predecessor CASC2D, the GSSHA model also includes the option to use the Richards equation to estimate changes in soil moisture, allowing for continuous simulations as well as single event simulations. For regions where snowmelt contributes significantly to runoff, GSSHA also includes a component for measuring snow accumulation and melting using an energy balance method. Ultimately, the GSSHA model's accuracy as a physically-based, distributed-parameter model, and its ability to simulate the hydrologic response of a watershed in a variety of different environments was the primary reason that it was selected for use in this project.

Downer and Ogden (2003) used the Goodwin Creek Experimental Watershed (GCEW) to verify GSSHA's ability to predict surface water runoff and estimate soil moistures in the unsaturated zone. GCEW is a small agricultural watershed located in northeastern Mississippi, where groundwater does not play a significant role in runoff

production and the chief runoff mechanism is infiltration-excess (Downer and Ogden, 2003). Researchers found that the model was able to reproduce peak discharges to within 31%, discharge volumes within 43%, and soil moisture profiles with a RMSE of 0.078 (Downer and Ogden, 2003).

Downer and Ogden (2004) again confirmed GSSHA's ability to predict surface water runoff, this time at the Muddy Brook watershed. Muddy Brook is a small watershed located in northeastern Connecticut which receives a large contribution of its runoff at the outlet from groundwater discharge and has a very shallow groundwater table (Downer and Ogden, 2004). Using GSSHA in this non-Hortonian basin, researchers were able to reproduce peak flows and total volumes within approximately 22% and 35%, respectively, of observed values (Downer and Ogden, 2004).

Sharif et al. (2010) explored the use of GSSHA to recreate an extreme flooding event that occurred in a sub-basin of the Guadalupe River in Texas, which is an area of the state that is known for being very prone to flash flooding. Researchers used precipitation inputs from both radar estimates and rain gages to drive the GSSHA model. At 1,630 km^2, the catchment area was relatively large as well as the simulation period of eleven days. The flood event had two main peaks, and researchers found that the GSSHA model was able to reproduce the two peak discharges with errors of 7.4% and 5.0%, respectively (Sharif et al., 2010).

3.2 Model Formulation

The major processes that are incorporated into the RHHMS hydrologic model include precipitation distribution, interception, infiltration, overland flow routing, and channelized flow routing. In developing the model, several key assumptions were made due to the intended implementation of the system in the arid and semi-arid western United States. One of the main assumptions made was that the primary runoff production mechanism is infiltration-excess. This can be expected from the type of intense convective thunderstorms that the region is known for, storms that are severe enough to produce a flash flood. Because soil moisture data was readily available at the testing location and because the model will ultimately have the use of real-time soil moisture sensors, evapotranspiration was not calculated. Finally, the interaction of groundwater flow was assumed to be negligible, as the depth to the groundwater table is typically very large in these arid and semi-arid regions. The formulas for each of the processes previously listed are explained below.

Precipitation Distribution

As there are a finite number of raingages and because the precipitation rate is not uniform across the watershed, the precipitation data that is recorded at each of the gages within the watershed must be interpolated throughout the ungaged areas in the watershed. To accomplish this, the inverse distance squared interpolation formula (Rojas, et al. 2003) was used and is shown in Equation (3.1) below:

$$r(t) = \frac{\sum_{m=1}^{n_g} \frac{r_m(t)}{d_m^2}}{\sum_{m=1}^{n_g} \frac{1}{d_m^2}} \tag{3.1}$$

where $r(t)$ is the calculated precipitation rate (in./hr) at the cell; n_g is the total number of raingages in the watershed; $r_m(t)$ is the precipitation rate (in./hr) recorded at the mth raingage; d_m is the distance (ft) from the current cell to the mth raingage.

Interception

The portion of rainfall that is intercepted by the vegetation cover is calculated using Gray's empirical 2-parameter method (Gray, 1970) which is shown in Equation (3.2) below:

$$\begin{aligned} int(t) &= r(t) \text{ for } I(t) < a \\ int(t) &= b * r(t) \text{ for } I(t) \geq a \end{aligned} \tag{3.2}$$

where $int(t)$ is the rate of interception (in./hr); a is the storage capacity (in.); b is the interception coefficient; $I(t)$ is the cumulative interception depth (in.). Storage capacity and interception coefficient values are estimated from land cover data (Downer and Ogden, 2006). These values can be found in Gray (1970) or Bras (1990). The calculated interception rate is then subtracted from the precipitation rate, yielding the net precipitation rate, $i(t)$, which is the precipitation value that is used in all subsequent calculations.

Infiltration

Neglecting the amount of surface ponding that occurs, the losses due to infiltration are then calculated using the Green-Ampt equation (Green and Ampt, 1911). This equation assumes that there is a sharp wetting front, and the soil above the wetting front is completely saturated. Initially, while the net precipitation rate is less than the saturated hydraulic conductivity, all of the water infiltrates and the rate of infiltration is simply equal to the net precipitation rate. Equations (3.3) and (3.4) calculate the infiltration rate and cumulative infiltration depth.

$$f(t) = i(t) \tag{3.3}$$

$$F(t) = F(t-1) + f(t) * dt \tag{3.4}$$

where $f(t)$ is the rate of infiltration (in./hr); $i(t)$ is the net precipitation rate (in./hr); $F(t)$ is the cumulative infiltration depth (in.) at the current time step; $F(t-1)$ is the cumulative infiltration depth (in.) in the previous time step; dt is the length of the time step (hr).

Once the net precipitation rate surpasses the saturated hydraulic conductivity, there is the potential for ponding to occur in the current time step. First, the infiltration depth at ponding is calculated in Equation (3.5). Next, the time to ponding is calculated in Equation (3.6). If the time to ponding does in fact fall within the current time step, the cumulative infiltrated depth is calculated using the Mein-Larson extension of the Green-Ampt equation (Mein and Larson, 1973). As the cumulative infiltration depth is located on both sides of Equation (3.8), it must be solved for using an iterative solution algorithm.

$$F_p = \frac{(n-\theta_i)\Phi_f}{\frac{i(t)}{K_s} - 1} \tag{3.5}$$

$$t_p = \frac{F_p - F(t-1)}{i(t)} + (t-1) * dt \tag{3.6}$$

$$t'_p = \frac{F_p - (n-\theta_i)\Phi_f \ln\left[1 + \frac{F_p}{(n-\theta_i)\Phi_f}\right]}{K_s} \tag{3.7}$$

$$F(t) = K_s\left(t - t_p + t'_p\right) + (n-\theta_i)\Phi_f \ln\left[1 + \frac{F(t)}{(n-\theta_i)\Phi_f}\right] \tag{3.8}$$

$$f(t) = \frac{F(t) - F(t-1)}{dt} \tag{3.9}$$

where F_p is the infiltration depth (in.) at ponding; n is the total porosity of the soil; θ_i is the initial soil moisture content; Φ_f is the wetting front suction head (in.); K_s is the soil saturated hydraulic conductivity (in./hr); t_p is the time (hr) at which the water begins to pond on the surface; t'_p is the equivalent time (hr) to infiltrate the cumulative infiltration depth at ponding, assuming initial surface ponding. The three soil parameters that are required for this equation, K_s, n, and Φ_f, can be found in Rawls et al. (1983). Initial soil moisture content must be measured in the field or estimated if necessary.

Overland Flow Routing

Overland flow is routed throughout the watershed using a form of the Manning equation to calculate the flow of water from cell to cell (Downer and Ogden, 2006). The following calculations apply to cells that are not located within the stream network. Initially, the surface is assumed to have no water accumulated, and the flow direction for

the first time step is calculated using the elevation data alone. For each following time step, the flow direction is updated using both the elevation and water depth of each neighboring cell. After calculating the friction slope in Equation (3.10), the flow of water from the current cell to its downstream neighbor is calculated in Equation (3.11) as:

$$S_f(t) = \left[\frac{z_i - z_{i+1}}{dx}\right] - \left[\frac{d_{i+1}(t) - d_i(t)}{dx}\right] \tag{3.10}$$

$$Q_i(t) = \frac{1.49}{n}\left(d_i(t)\right)^{5/3}\left(S_f(t)\right)^{1/2} \tag{3.11}$$

where $Q_i(t)$ is the flow (ft^3/s) leaving the cell at the current time step; n is the Manning roughness coefficient of the cell; $d_i(t)$ is the depth of water (ft) in the current cell; $d_{i+1}(t)$ is the depth of water (ft) in the downstream cell; $S_f(t)$ is the friction slope between the current cell and the downstream cell; z_i is the elevation (ft) of the current cell, z_{i+1} is the elevation (ft) of the downstream cell; dx is the grid cell size (ft).

Water depth in the next time step is then calculated using Equation (3.12) by subtracting the losses from infiltration and the flow leaving the cell, as well as adding the precipitation inputs and the flow coming into the cell from any neighboring cells that flow into the cell.

$$d_i(t+1) = d_i(t) + \left[(dt) * \left(i(t) - f(t)\right)\right] + \left[\left(Q_{i-1}(t) - Q_i(t)\right) * \left(\frac{3600 * dt}{dx^2}\right)\right] \tag{3.12}$$

where $d_i(t+1)$ is the depth of water (ft) in the cell at the next time step; $Q_{i-1}(t)$ is the flow (ft^3/s) entering the cell from any of the eight neighboring cells.

If at any time the friction slope is negative causing the flow to move upstream, the flow rate at the current cell is calculated in Equation (3.13) using the parameters of the downstream cell, with the resulting flow rate being a negative value.

$$Q_i(t) = -\left[\frac{1.49}{n}\left(d_i(t)\right)^{5/3}\left(\left|S_f(t)\right|\right)^{1/2}\right] \tag{3.13}$$

Channelized Flow Routing

When the surface flow reaches a defined channel network, the Manning equation is again used to relate the water depth to discharge, this time in a slightly altered form shown in Equation (3.14) below (Downer and Ogden, 2006).

$$Q_i(t) = \frac{1.49}{n}\left(A(t)\right)\left(R(t)\right)^{2/3}\left(S_f(t)\right)^{1/2} \tag{3.14}$$

where $A(t)$ is the cross-sectional area (ft²) of the channel; $R(t)$ is the hydraulic radius (ft²/ft) of the channel.

The volume of the cell at the next time step is then calculated using Equation (3.15) in a manner similar to the overland flow depth calculation, and finally the water depth is obtained from this volume as shown in Equation (3.16).

$$\begin{aligned} V_i(t+1) = V_i(t) &+ \left[dt * dx^2 * \left(i(t) - f(t)\right)\right] \\ &+ \left[3600 * dt * \left(Q_{i-1}(t) - Q_i(t)\right)\right] \end{aligned} \tag{3.15}$$

$$d_i(t+1) = \frac{-b + \sqrt{(b^2) - 4(Z)\left(-\frac{V_i(t+1)}{dx}\right)}}{2(Z)} \tag{3.16}$$

where $V_i(t+1)$ is the volume (ft^3) of water in the cell at the next time step; $V_i(t)$ is the volume (ft^3) of water in the cell at the current time step; b is the bottom width (ft) of the channel; Z is the side slope of the channel (horizontal distance/vertical distance).

3.3 Model Inputs and Preprocessing

In order to run simulations using the RHHMS hydrologic model, numerous datasets must be assembled as well as several input parameter values. The model is driven by gaged precipitation and soil moisture data gathered from instruments in the field. The hydrologic and topographic information used in the model can been extracted from GIS digital spatial data and digital elevation models. All of the datasets described herein can be created using a GIS and must be converted into an ASCII map. Table 3.1 lists the basic inputs and Table 3.2 lists the necessary datasets that are required.

Table 3.1. Model Required Inputs

Input	Type	Units	Description
dx	Double	ft	Grid cell size.
Wr	Integer	-	Total number of rows in the grid.
Wc	Integer	-	Total number of columns in the grid
NT	Integer	-	Total number of overall model time steps.
NF	Integer	-	Total number of flow routing time steps.
dt	Double	hr	Length of overall model time step.
df	Double	hr	Length of flow routing time step.
Ngages	Integer	-	Total number of raingages.
EndData	Integer	-	Total number of rows of raingage data.

Table 3.2. Model Required Datasets

Dataset Name	Type	Units	Description
Elevation	Double	ft	ASCII map containing the elevation of each grid cell. Must be adjusted if any imperfections exist in the DEM.
Watershed Boundary	Boolean	-	ASCII map containing the watershed status of each grid cell. Cells inside the watershed are assigned a value of 1. Cells outside of the watershed are assigned a value of 0.
Gage Locations	Integer	-	ASCII map containing the location of each raingage as well as the outlet cell location. Cells containing a raingage are assigned a value of 2. Outlet cell assigned a value of 3.
Gage Data	N/A	in.	Spreadsheet containing precipitation inputs from each gage. Must include gage number, start time, duration, and precipitiation depth.
Flow Direction	Integer	-	ASCII map containing the initial flow direction of each grid cell.
Saturated Conductivity	Double	in./hr	ASCII map containing the value of the saturated hydraulic conductivity of each grid cell.
Wetting Front Suction Head	Double	in.	ASCII map containing the value of the Green-Ampt wetting front suction head of each grid cell.
Porosity	Double	decimal	ASCII map containing the value of the soil porosity of each grid cell.
Initial Soil Moisture	Double	decimal	ASCII map containing the value of the initial soil moisture content of each grid cell.
Manning's n	Double	-	ASCII map containing the value of the Manning roughness coefficient of each grid cell.
Stream Network	Boolean	-	ASCII map containing the stream network location. Cells that are part of the stream network are assigned a value of 1. All other cells assigned a value of 0.
Bottom Width	Double	ft	ASCII map containing the value of the channel bottom width of each grid cell located in the stream network.
Z	Double	-	ASCII map containing the value of the average channel side slope (horizontal:vertical) of each grid cell located in the stream network.
Storage Capacity	Double	in.	ASCII map containing the value of Gray's interception storage capacity of each grid cell.
Interception Coefficient	Double	-	ASCII map containing the value of Gray's interception coefficient of each grid cell.

The precipitation data used in the model can be gathered from gages located both within and surrounding the watershed of interest. While the fully operational RHHMS will have the use of a network of recording raingages, gaged precipitation data can be accessed from the National Oceanic and Atmospheric Administration (NOAA) National Climatic Data Center (NOAA, 2012). A gage location map must be created which defines the location of each raingage in the watershed, as well as the outlet cell. In this map, each cell that contains a raingage is assigned a value of 2 and the outlet cell is assigned a value of 3, all other cells being assigned a no-data value or a value of 0. An example of the gage location map is shown in Figure 3.1. The model also requires the initial soil moisture content for each grid cell. Values for initial soil moisture must be established from gaged data if available or estimated if not. The total number of raingages that are utilized also needs to be specified upfront.

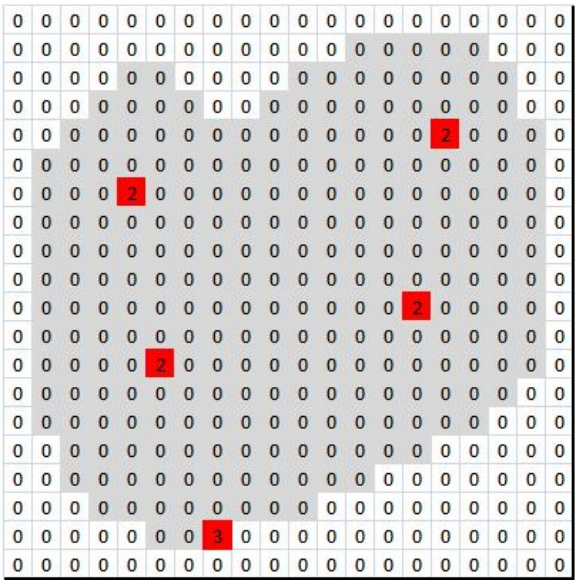

Fig. 3.1. Example of Gage Location Map

Prior to creating required input grids, the user must first select a grid cell size. This will depend on the size of the watershed as well as the resolution of the available parameter data. For example, if a 30 meter DEM is used as the elevation input data, obviously a grid cell size of 30 meters or larger should be selected. Also, if the watershed of interest is, for example, an entire river basin, the grid cell size will have to be quite large in order to have a reasonable computation time. The grid cell sizes used in the GSSHA model normally range from 10 to 250 m (Downer and Ogden, 2006). Another very important parameter that must be determined before running model simulations is the length of the model time step as well as the length of the flow routing time step. The overall model time step length will typically be set according to the quality of the precipitation data that is used.

Elevation data used in the model is available nationwide from the USGS National Elevation Dataset (NED) Program (USGS, 2011a). This data typically contains errors that must be accounted for before it can be used for modeling. Errors in spatial data often cannot be avoided, and can be due to the age of the data, an incomplete sampling density, processing errors in the computer, as well as measurement errors including positional imprecision or data entry errors (Wechsler, 2007). DEMs may also contain natural depressions known as “sinks” or “pits” that must be filled before overland flow routing can be calculated. Once corrected, DEMs contain useful information that can lead to the creation of other datasets including flow direction maps, stream locations, and watershed boundary maps using tools available in GIS software

such as ArcGIS (Environmental Systems Research Institute (ESRI), Redlands, California).

The flow direction map is used to route flow for the initial time period in which there is no surface water accumulation, and consists of a grid in which each cell is assigned a number corresponding to the direction of one of its eight adjacent "neighbor" cells. Figure 3.2 defines the values corresponding to the eight possible flow directions.

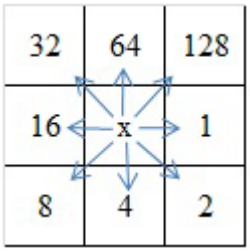

Fig. 3.2. Flow Direction Values

The flow direction of each cell is first determined using only the elevation data, in which the flow moves from the current cell to the cell that results in the steepest slope. As surface water begins accumulating, these initial flow direction values are subject to change and the flow direction is then determined based on the drop in total head. The watershed boundary map is a Boolean map in which each grid cell located within the watershed is assigned a value of 1, and all other cells in the grid are assigned a value of 0. Figure 3.3 demonstrates an example of the watershed boundary map.

0	0	0	0	0	0	0	0	0	0	0	0	0	0	0	0	0	0	0	0
0	0	0	0	0	0	0	0	0	0	0	0	1	1	1	1	1	0	0	0
0	0	0	0	1	1	0	0	0	0	1	1	1	1	1	1	1	1	0	0
0	0	0	1	1	1	1	0	0	1	1	1	1	1	1	1	1	1	0	0
0	0	1	1	1	1	1	1	1	1	1	1	1	1	1	1	1	1	1	0
0	1	1	1	1	1	1	1	1	1	1	1	1	1	1	1	1	1	1	0
0	1	1	1	1	1	1	1	1	1	1	1	1	1	1	1	1	1	1	0
0	1	1	1	1	1	1	1	1	1	1	1	1	1	1	1	1	1	1	0
0	1	1	1	1	1	1	1	1	1	1	1	1	1	1	1	1	1	1	0
0	1	1	1	1	1	1	1	1	1	1	1	1	1	1	1	1	1	1	0
0	1	1	1	1	1	1	1	1	1	1	1	1	1	1	1	1	1	1	0
0	1	1	1	1	1	1	1	1	1	1	1	1	1	1	1	1	1	1	0
0	1	1	1	1	1	1	1	1	1	1	1	1	1	1	1	1	1	1	0
0	1	1	1	1	1	1	1	1	1	1	1	1	1	1	1	1	1	0	0
0	1	1	1	1	1	1	1	1	1	1	1	1	1	1	1	1	0	0	0
0	0	1	1	1	1	1	1	1	1	1	1	1	1	1	0	0	0	0	0
0	0	1	1	1	1	1	1	1	1	1	1	1	0	0	0	0	0	0	0
0	0	0	1	1	1	1	1	1	1	1	0	0	0	0	0	0	0	0	0
0	0	0	0	0	1	1	1	0	0	0	0	0	0	0	0	0	0	0	0
0	0	0	0	0	0	0	0	0	0	0	0	0	0	0	0	0	0	0	0

Fig. 3.3. Example Watershed Boundary Map

Soils data required for model can be downloaded from the USDA National Resources Conservation Service (NRCS) website (USDA, 2011). These data can be used to estimate initial values for the watershed infiltration parameters including saturated hydraulic conductivity, porosity, and wetting front suction head.

Land cover data required for the model can be downloaded from the National Land Cover Database (MRLC, 2011). These data can be used to estimate initial values for the Manning roughness coefficient, interception storage capacity, and interception coefficient.

Data describing surface water features such as rivers and streams can be downloaded from the National Hydrography Dataset (USGS, 2011b). This data can be used to define the stream network in the watershed. There are several methods of defining the stream network and creating a stream network map. One method is to

overlay the stream map from the hydrography data and simply convert the data from its vector form to a raster map. Another method is to create a flow accumulation map for the watershed and define the number of cells that must be accumulated for a cell to be considered a stream cell. Once the stream network is defined, a Boolean map must be created in which a stream cell is assigned a value of 1 and all other cells a value of 0. Figure 3.4 shows an example of the stream network map.

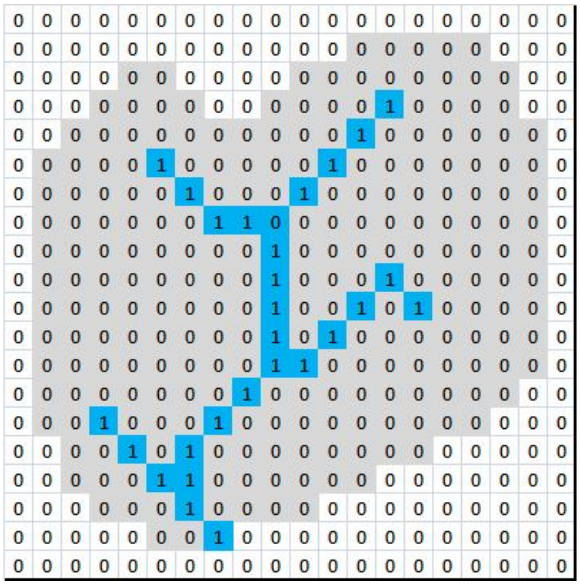

Fig. 3.4. Example Stream Network Map

Perhaps the most important input data that are required to achieve accurate model simulations are the channel cross-sectional data. These are also usually the hardest data to locate. Typically, a survey of the watershed is required to gather this data, however, if adequate LIDAR elevation data exists, this information can be obtained through data

processing programs such as HEC-GeoRAS (Hydrologic Engineering Center (HEC), Vicksburg, Mississippi).

3.4 Model Calibration and Validation

The RHHMS hydrologic model was calibrated manually using 5 recorded storm events at the WG-11 sub-watershed of WGEW. Information on each of the storm events is shown in Table 3.3.

Table 3.3. Calibration and Validation Storm Events

Event No.	Event Date	Storm Start Time	Flow Start Time	Flow Duration (min)	Peak Flow Rate (ft^3/s)	Total Flow Volume (ft^3)	Average Rainfall Depth (in.)	Gage Standard Deviation
C1	7/20/2007	18:26	18:58	203	674	1,129,000	1.93	0.355
C2	7/19/2008	20:50	21:42	90	96	149,500	1.20	0.344
C3	8/25/2003	11:58	12:16	156	40	106,100	0.43	0.423
C4	8/16/2010	17:04	17:11	139	291	627,600	0.86	0.437
C5	8/28/2010	14:19	14:34	199	225	640,900	0.85	0.242
V1	8/23/2009	13:28	14:00	158	152	296,900	0.97	0.197
V2	8/4/2002	12:12	12:32	165	310	550,200	0.97	0.428
V3	7/31/2007	14:54	15:17	119	234	434,300	0.80	0.784
V4	8/6/2007	17:02	17:09	296	122	535,500	0.93	0.560
V5	8/28/2008	12:50	13:07	303	132	560,900	1.01	0.592

The WG-11 sub-watershed encompasses approximately 7.8 km^2 and contains a total of 9 digital raingages within the watershed boundary, as well as a flume at the outlet. Nine digital raingages outside of the watershed, but in close proximity, were also used to provide data to the model, combining for a total of 18 raingages. A portion of the

watershed was not used in the modeling calculations as it is a stock pond watershed that has been determined to not significantly contribute to runoff at the outlet in the majority of previous studies that have utilized this site. A map of the WG-11 sub-watershed, as well as the entire model grid can be seen in Figure 3.5 below. A soils map of WG-11 is depicted in Figure 3.6, along with each soil name listed in Table 3.4.

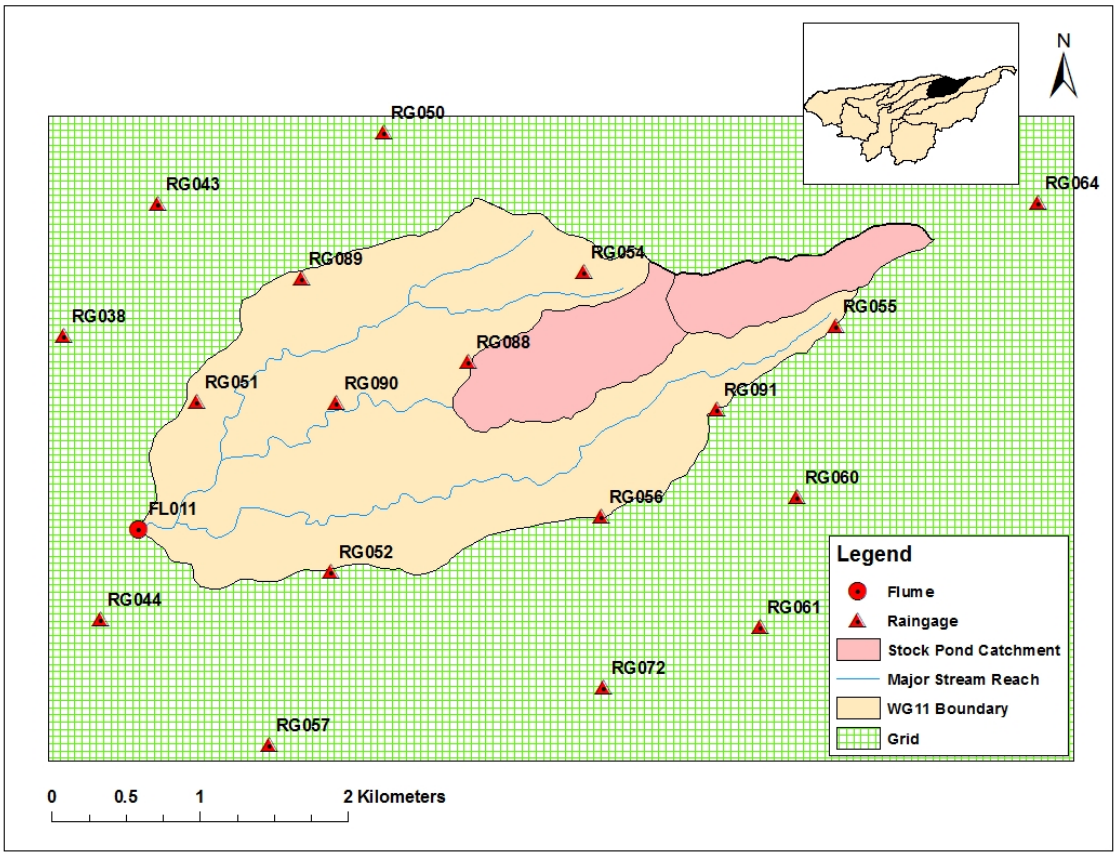

Fig. 3.5. Sub-watershed WG-11 Site Map

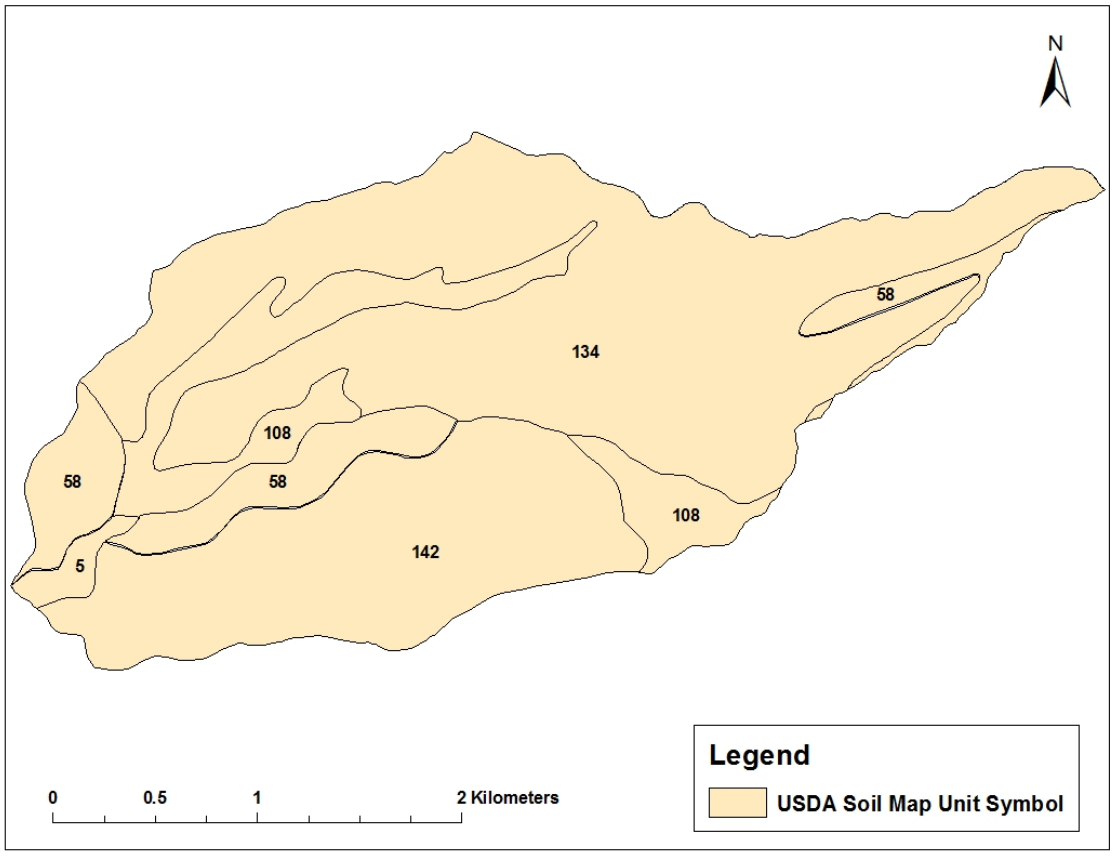

Fig. 3.6. WG-11 Soils Map

Table 3.4. WG-11 Soil Types

Map Unit Symbol	USDA Soil Map Unit Name
5	Baboquivari-Combate complex, 0 to 3 percent slopes
58	Elgin-Stronghold complex, 3 to 20 percent slopes
108	McAllister-Stronghold complex, 3 to 20 percent slopes
134	Stronghold-Bernardino complex, 10 to 30 percent slopes
142	Tombstone very gravelly fine sandy loam, 8 to 15 percent slopes

The digital spatial data that was used in the calibration and validation processes, including elevation, soils, land cover, hydrography, and gage location data, were downloaded from the SWRC online data catalog (USDA-ARS, 2012). While channel cross-sectional data for the sub-watershed were not accessible online, KINEROS cross-sectional input files that included the channel bottom width and channel side slopes were provided by Dr. David Goodrich of the SWRC, from work completed on an earlier project (2012, USDA-SWRC, personal communication).

A grid cell size of 50 m was selected for both the calibration and validation processes in order to fully define the geometry of the channel network. As precipitation data was available in one-minute intervals for almost all of the storms, a relatively small model time step of 6 min was selected to model each of the storms. The flow routing time step that was selected was very small, at approximately 1.5 sec. Initial soil moisture values for the site were determined using data from a soil moisture sensor located near the center of the watershed.

The calibration parameters for each of the five storm events included the Manning roughness coefficient, soil saturated hydraulic conductivity, wetting front suction head, porosity, interception storage capacity, and interception coefficient. Initial values of the calibration parameters were estimated using values from the literature (Gray, 1970; Rawls et al., 1983) and are shown in Table 3.5 below. These initial values were manually calibrated independently for each storm event by applying a multiplier to each parameter until the modeled hydrograph best resembled the actual recorded hydrograph. These multipliers were determined for each of the five calibration storm

events, and the average value of the calibration parameter multipliers was then applied to the parameters for each of the validation set of storms.

Table 3.5. Calibration Parameters

Calibration Parameter	WG-11 Initial Parameter Value Range	Units	Average Calibration Parameter Multiplier
Manning Roughness Coefficient	0.045-0.055	-	0.68
Saturated Hydraulic Conductivity	0.06-2.18	in./hr	0.79
Wetting Front Suction Head	8.89-31.63	in.	0.79
Total Porosity	0.33-0.434	-	0.96
Interception Storage Capacity	0.005-0.01	in.	1.10
Interception Coefficient	0.08-0.16	-	1.10

3.5 Model Limitations and Uncertainty

It is important to remember that a model is simply an approximation of reality, and can never completely describe the spatial heterogeneity of the watershed or the complex nature of the hydrologic processes that present in the system in which it is applied with absolute exactitude and certainty. As the RHHMS hydrologic model is tailored toward a specific type of storm event in a specific region, this allowed the use of many assumptions, thereby resulting in the potential for a high level of uncertainty. If not properly applied, there is a large potential for error in this model.

Once again, the intended goal of this model is to predict the runoff from extreme storm events, the likes of which are capable of producing flash floods, in arid and semi-arid regions. This allows for the assumption that the Hortonian infiltration-excess

mechanism is the dominant runoff production mechanism, and that the interaction of groundwater to runoff is negligible. These assumptions generate one of the more significant sources of uncertainty in the model. The model is not intended to be used on storm events with a lower intensity, in which the saturation-excess runoff mechanism is dominant, or in areas where groundwater contributes a significant amount to runoff.

Other sources of uncertainty in this model include the trapezoidal simplification of the channel geometry, as well as the assumption of steady, uniform flow conditions implied by the use of Manning's equation. In reality, the geometry of a channel network is highly variable from one cross section to the next, and these natural streams rarely exhibit uniform flow. The amount of error from this assumption can be minimized, however, with a reduction in grid cell size. As the distance from one cell to the next decreases, so too does the change in channel cross section geometry and flow conditions.

Finally, the extreme spatial variability of both the parameter data as well as the precipitation inputs provides another source of uncertainty in the modeling process. In a perfect world, each watershed would be completely instrumented and have accurate elevation, soils, and land use data for every square inch of the basin. This of course, is usually far from the truth. As mentioned previously, even distributed-parameter models are limited by the resolution and quality of the parameter data that is available, therefore making them lumped to a certain degree. The use of a relatively large grid cell size, as well as the estimations that were made as to the initial parameter values contributes a significant amount of uncertainty to the modeling process. Likewise, the spatial variability of the storm events themselves and the lack of complete raingage coverage

also contribute significantly to the model uncertainty. The calibration and validation storm events that were used in this study produced highly dissimilar precipitation depths from one gage to the next. While there currently exists no method of completely capturing the spatial variability of each storm event, one of the goals of this research is to find a way to minimize these potential errors, and provide the best possible input data.

3.6 Results and Analysis

Three basic hydrograph metrics were used to compare the performance of the modeled hydrographs to the actual recorded hydrographs for both the calibration and validation storms, including the percent error in peak flow rate, the difference in runoff peak timing, and the percent error in the total volume of runoff. A summary of the results of the calibration and validation processes can be seen in Table 3.6 below. The resulting hydrographs of each of the calibration and validation event simulations can be found in Figures 3.7-3.16.

Table 3.6. Calibration and Validation Results

Event No.	Peak Flow Error (%)	Δt_p (min)	Total Volume Error (%)
C1	2.3	0	30.8
C2	-0.4	0	118.0
C3	0.0	0	48.5
C4	1.0	6	-23.3
C5	0.5	6	-3.9
V1	-31.0	-12	-0.7
V2	1.5	6	31.4
V3	1.6	12	31.2
V4	-54.6	-6	-48.4
V5	-22.0	-24	-52.3

For the five calibration storms, after adjusting the initial input parameter values the RHHMS hydrologic model was able to reproduce peak discharge, peak timing, and total runoff volume with average errors of 0.8%, 2.4 min, and 44.9%, respectively. Errors in peak discharge from the model simulations ranged from a minimum of 0.02% to a maximum of 2.3%. Errors in peak timing ranged from a minimum of 0 min to a maximum of 6 min. Finally, errors in total volume from the calibration set of storm events ranged from a minimum of 3.9% to a maximum of 118%.

After calibrating each storm event individually by adjusting the model parameters until the modeled peak discharge best fit the recorded peak discharge, an average of the parameter values used in the five calibration storm events was used to model the five validation storm events. For the five validation storm events, it was found that the model was able to reproduce peak discharge, peak timing, and total volume with

an average error of 22.1%, 12 min, and 32.8%, respectively. Errors in peak discharge ranged from a minimum of 1.5% to a maximum of 54.6%. Errors in peak timing ranged from a minimum of 6 min to a maximum of 24 min. Finally, errors in total runoff volume over the set of validation storm events ranged from a minimum of 0.7% to a maximum of 52.3%.

Looking at the individual validation storm events, there are several likely explanations for the error in the modeled peak discharge. The model underestimated the peak discharge of storm V1 by 31%, and calculated a peak timing that occurred 12 min sooner than the actual time. This is most likely due to an underestimation in the roughness coefficient, which would create an increase in velocity and a lower peak flow rate.

While the model calculated the peak discharge in storm events V2 and V3 with negligible error, it overestimated the total volume of runoff by approximately 31% for both storm events. This is most likely due to infiltration parameters or interception parameters that were too low, causing an underestimation in abstractions. The modeled peak timings for storm events V2 and V3 occurred 6 min and 12 min later than the actual time, respectively. This could be explained by a roughness coefficient that was too high, creating a slower flood peak that was greater in magnitude.

Conversely, the model underestimated the peak discharge of storm events V4 and V5 by 54.6% and 22%, respectively. The model also underestimated the total runoff volume by 48.4% and 52.3%, respectively. This could be due to infiltration and interception parameters that were too high, resulting in an overestimation in abstractions.

The modeled peak timing for storm events V4 and V5 occurred 6 min and 24 min sooner than the actual time, respectively. This is most likely due to roughness coefficients that were too low, which would explain not only the underestimation in peak timing but also the underestimation in peak discharge for each of these simulations.

Overall, the calibrated model was able to reproduce the peak discharge, peak timing, and total runoff volume of the five validation storm events to within an average of 22.1%, 12 minutes, and 32.8%, respectively. While these numbers are certainly not ideal, the model provides an acceptable starting point for subsequent versions and the results can be used to further improve the model and examine possible sources of error that exist.

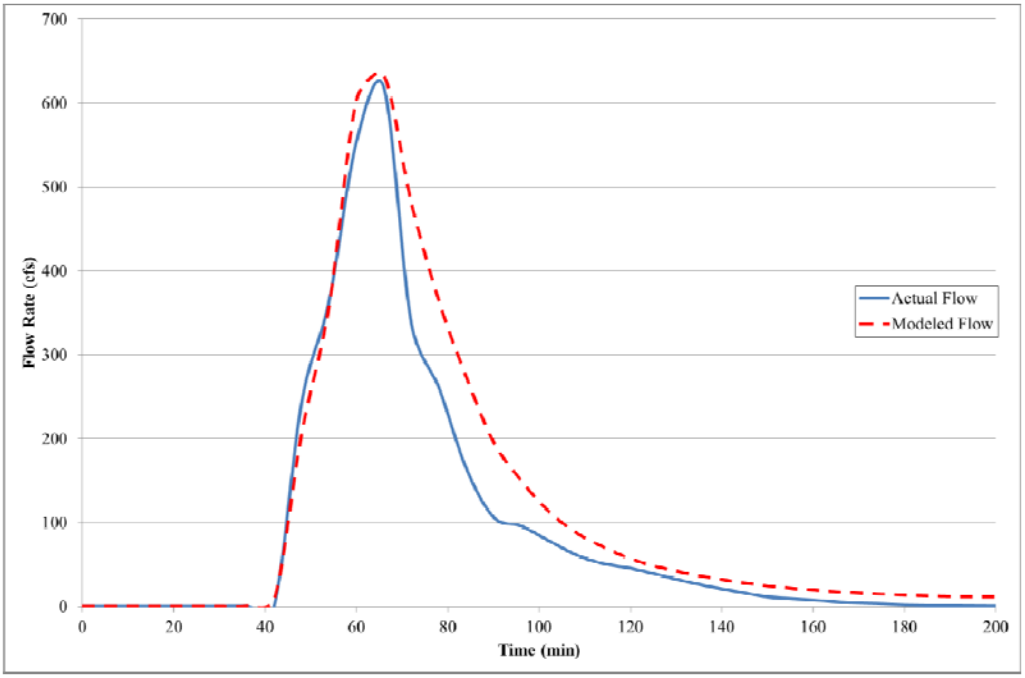

Fig. 3.7. Calibration Event C1 Hydrograph

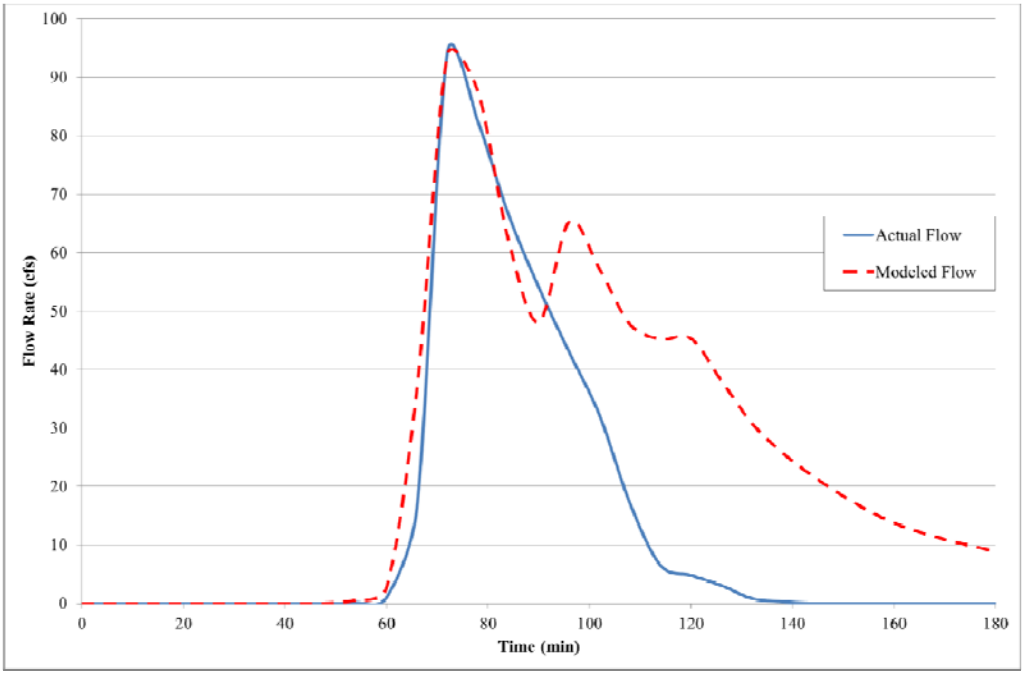

Fig. 3.8. Calibration Event C2 Hydrograph

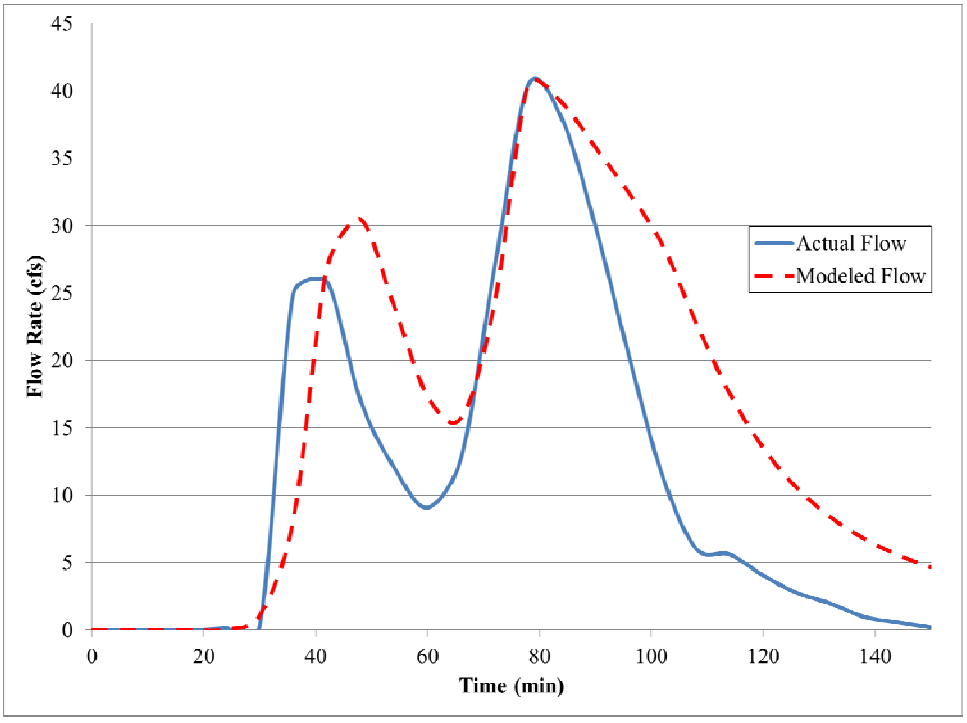

Fig. 3.9. Calibration Event C3 Hydrograph

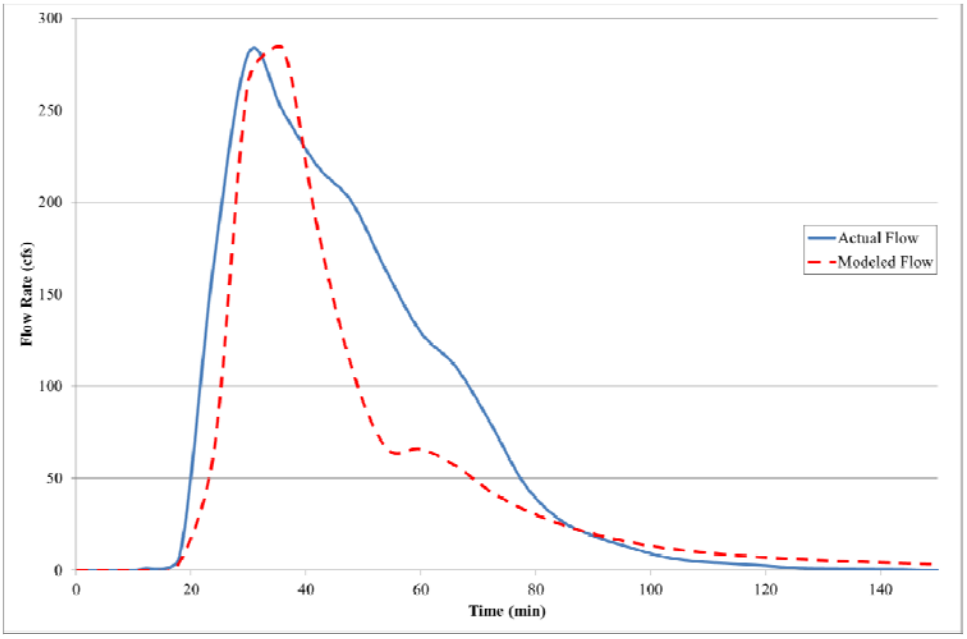

Fig. 3.10. Calibration Event C4 Hydrograph

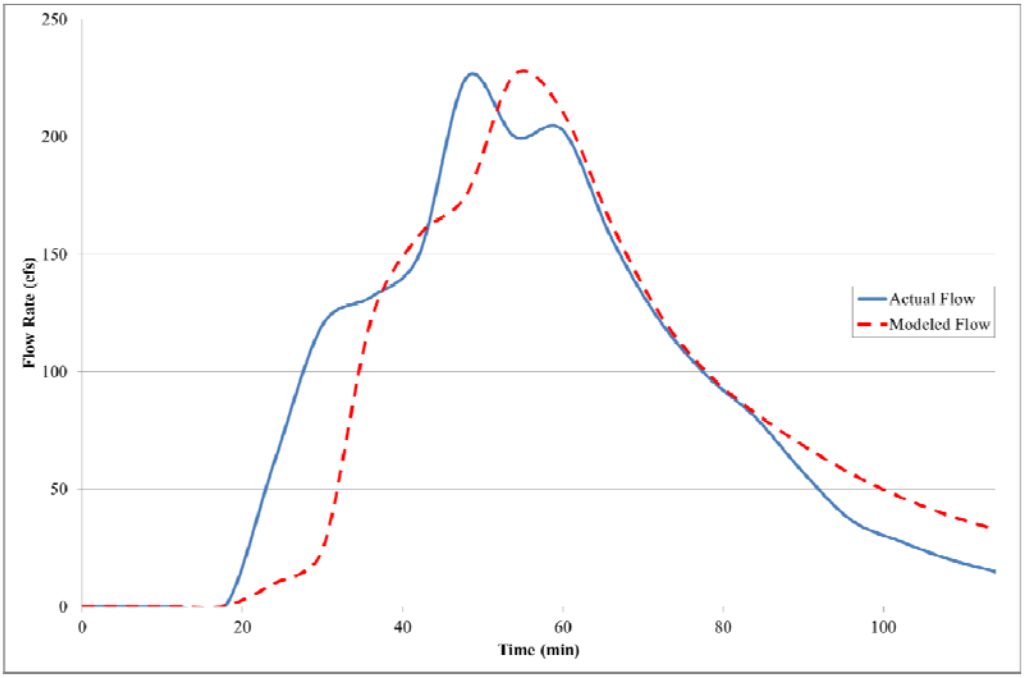

Fig. 3.11. Calibration Event C5 Hydrograph

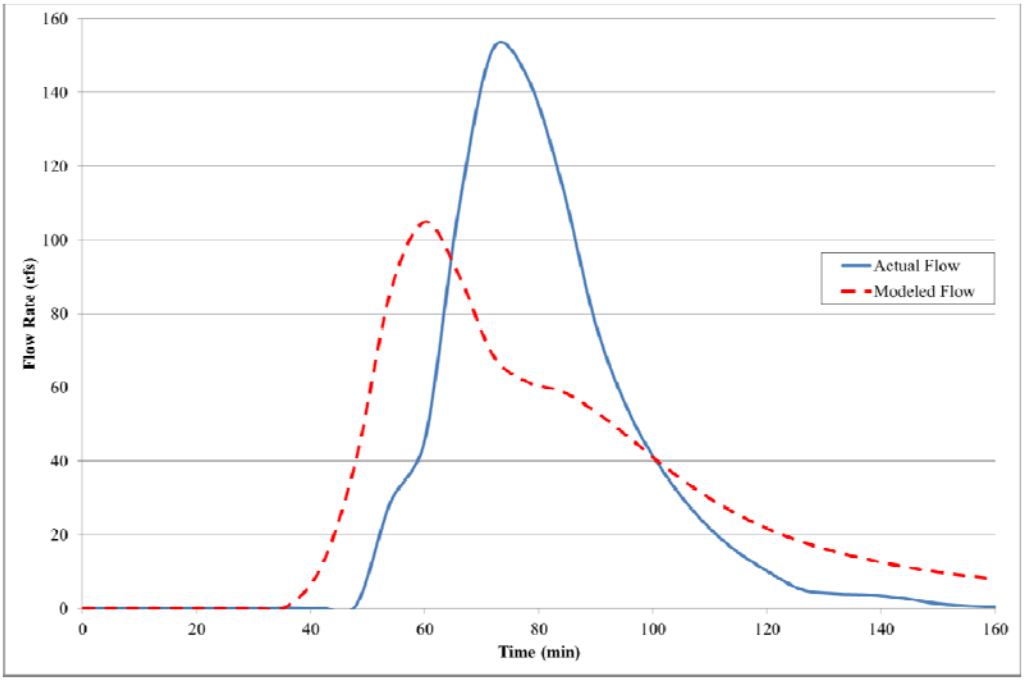

Fig. 3.12. Validation Event V1 Hydrograph

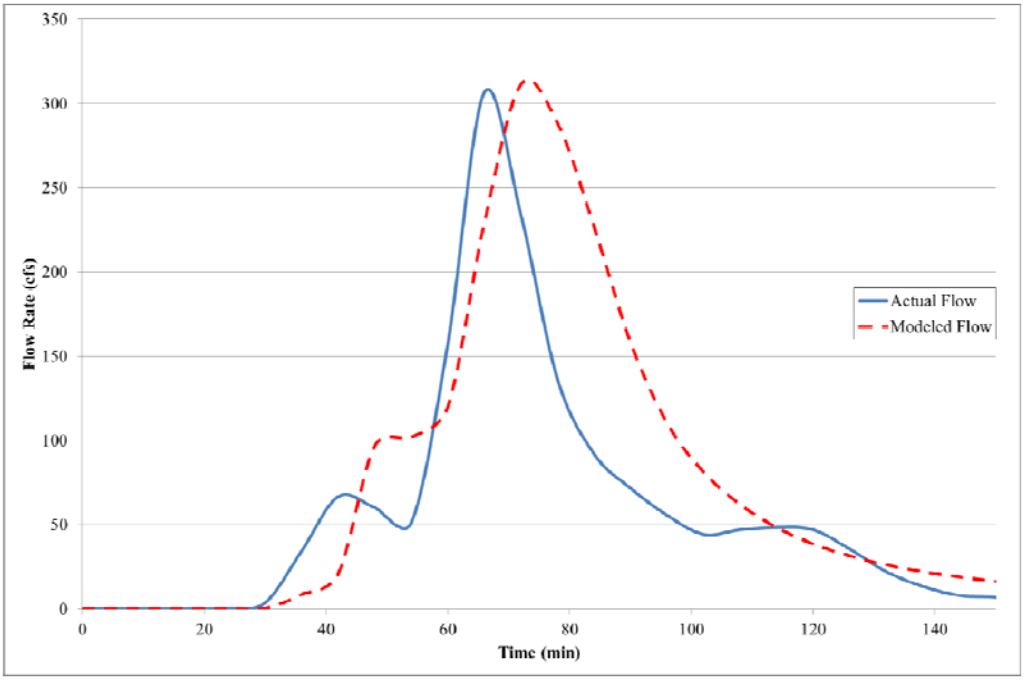

Fig. 3.13. Validation Event V2 Hydrograph

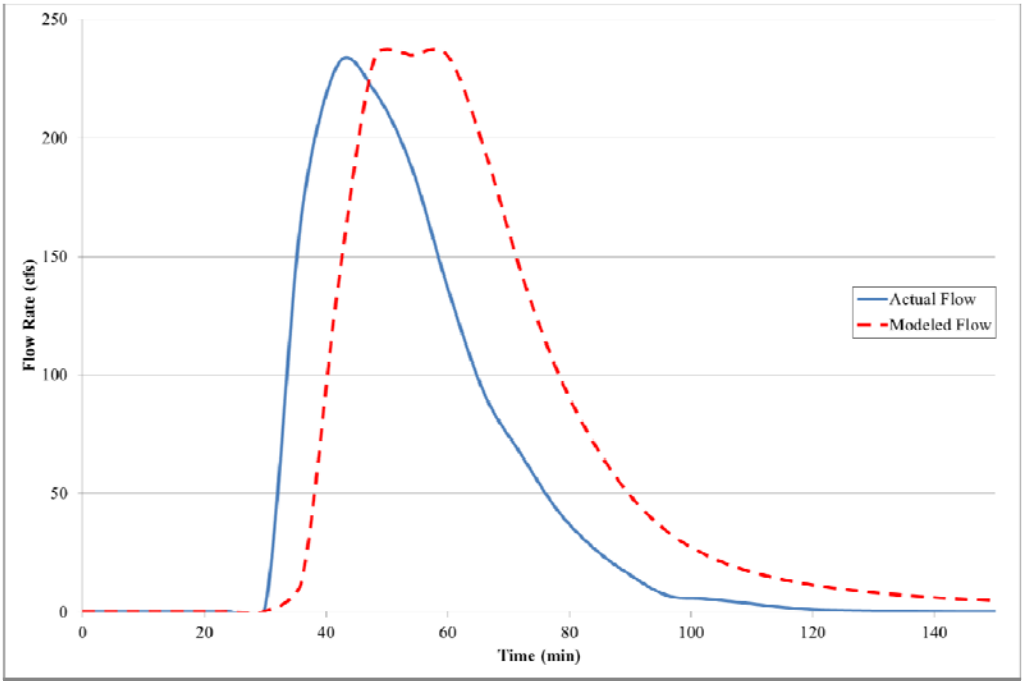

Fig. 3.14. Validation Event V3 Hydrograph

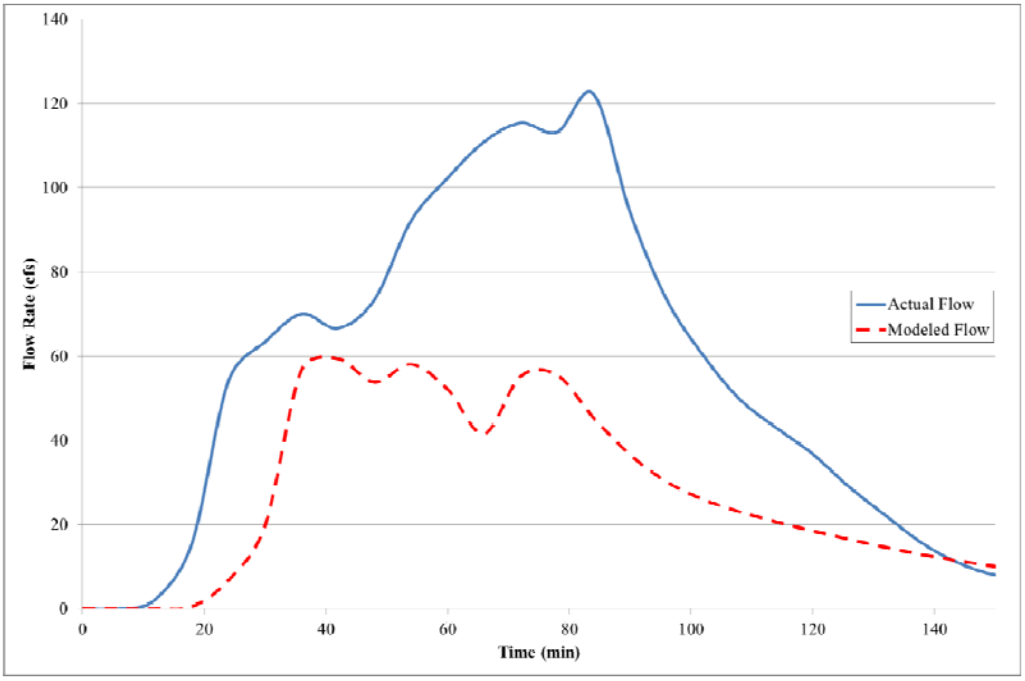

Fig. 3.15. Validation Event V4 Hydrograph

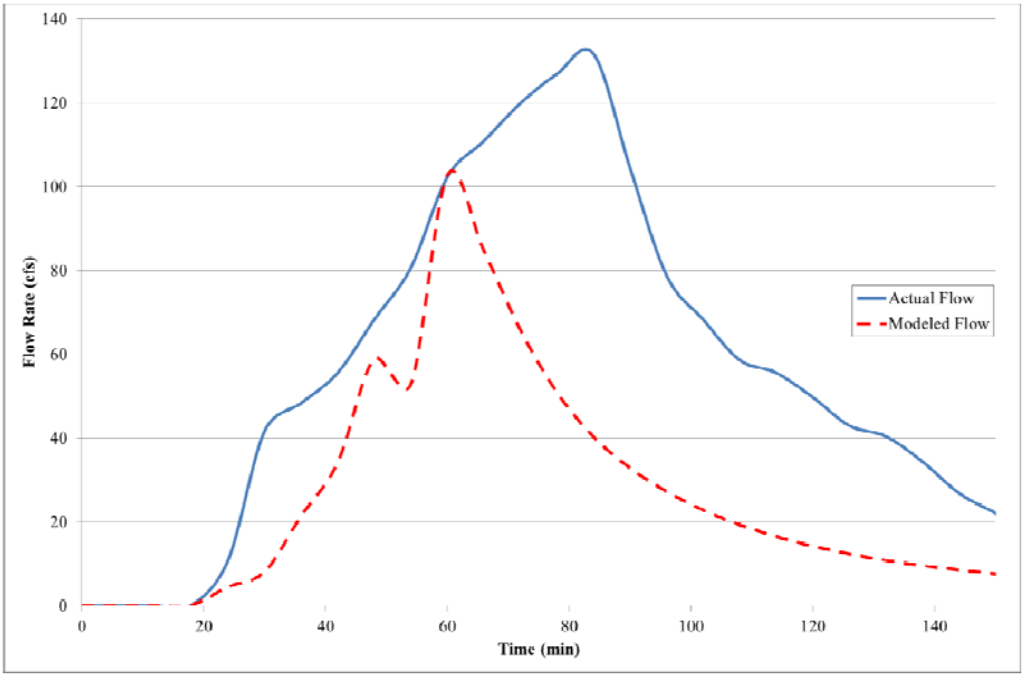

Fig. 3.16. Validation Event V5 Hydrograph

4. GAGE DENSITY REDUCTION: COMPARISON WITH MODEL ACCURACY

4.1 Summary

As stated previously, one of the main objectives of this project is to identify a methodology for determining both the placement location, as well as the minimum density of raingages to deploy, while still remaining capable of providing adequate inputs to the hydrologic model, and yielding runoff predictions with an acceptable level of accuracy. Raingages are not inexpensive, both in regard to the initial cost of the instruments as well as the cost of maintaining the instruments and keeping the system functioning properly. While an enormous network of sensors containing a raingage in each model grid cell would be ideal, the cost as well as the man hours spent assembling and maintaining the network would be tremendous. Furthermore, Osborn et al. (1972) points out that the trails required to access the gages could significantly alter the terrain, thereby changing the drainage of a watershed. At the other extreme, having just one or very few gages in a relatively large watershed would involve a low cost, but would most likely be unable to accurately convey the high spatial variability of most storms, especially the convective thunderstorms that the arid and semi-arid western U.S. is known for. As such, a methodology is needed to determine the minimum number of gages must be used, as well as where these gages should be located in order to best capture the spatial variability of the storm events.

Osborn et al. (1972) used data from summertime convective thunderstorms at WGEW to determine the optimum rain gage density needed to accurately correlate rainfall and runoff. Researchers ultimately found that in order to accurately predict runoff, the follow gage networks are required:

- small watersheds with an area no larger than 120 acres require one centrally located gage,
- a watershed with an area of 1 mi^2 and a length-width ratio of 4 requires a network of three evenly spaced gages, and
- large watersheds with an area of over 10 mi^2 require a network of evenly spaced gages at 1.5 mile intervals.

4.2 Methodology

The vast network of raingages at the WGEW proved to be an ideal testing site to develop the gage network reduction procedure. A data censoring study was performed using the same site in which the calibration and validation processes were carried out. Initially, all of the available rain gages in the test watershed were used to provide inputs to the hydrologic model, serving as the control case in this experiment. Later, the number of gages that were utilized was reduced, and the resulting model performance was analyzed. The goal in this effort is determine a way to find not only the minimum number of gages to deploy, but also determine where these gages should be located in order to accurately capture the spatial heterogeneity of the convective thunderstorms of the region. This will also give some clue as to the tradeoff between the cost and scope of

a sensor network, versus its prediction accuracy, and help to determine the ideal gage placement density when it comes time to implement the fully operational RHHMS in the field.

The WG-11 sub-watershed of WGEW was again used in the data censoring study. Two storm events, V2 and V3, were selected to drive the simulations. These storm events were selected due to their high spatial variability and also because they best reproduced the actual peak discharges out of all of the validation storm event simulations. For each of the two storm events, 5 different cases were simulated. Case 1 was the control case, in which the model was run using inputs from all of the 18 raingages that were used in the calibration and validation of the model. For Case 2, a "medium" number of gages were utilized, and the number of raingages providing inputs to the model was reduced by 50%, resulting in a total of 9 raingages. These gages were selected on a random basis for each of 15 samples. Case 3 again used the medium number of 9 raingages, which were this time selected based on a minimization of correlation method described below.

For each of the 18 raingages, the total precipitation depths recorded for each of the 10 calibration and validation storms were calculated and placed into an array as shown in Table 4.1. Next, the sample correlation coefficient for each pair of gages was determined using Equation (4.1) below (Devore, 2009):

$$Corr(\mathrm{X},\mathrm{Y}) = \frac{\sum_{i=1}^{n}(x_i - \bar{x})(y_i - \bar{y})}{\sqrt{\sum_{i=1}^{n}(x_i - \bar{x})^2}\sqrt{\sum_{i=1}^{n}(y_i - \bar{y})^2}} \tag{4.1}$$

where $Corr(\mathrm{X},\mathrm{Y})$ is the sample correlation coefficient; X is the array of precipitation depths recorded for each storm event at the first gage; Y is the array of precipitation depths recorded for each storm event at the second gage; n is the total number of storm events used; x_i is the precipitation depth recorded at the first gage during the i^{th} storm; y_i is the precipitation depth recorded at the second gage during the i^{th} storm; $\bar{x}$ is the mean precipitation depth recorded at the first gage; $\bar{y}$ is the mean precipitation depth recorded at the second gage.

Table 4.1. Precipitation Depths at Individual Raingages

Gage No.	Precipitation Depth (in.) for Selected Storm Event									
	C1	C2	C3	C4	C5	V1	V2	V3	V4	V5
38	1.385	1.160	0.715	0.085	0.825	0.715	1.860	2.310	0.165	0.365
43	1.615	0.990	0.165	0.690	0.515	0.955	1.235	2.095	0.265	0.300
44	1.485	1.680	0.910	0.500	0.880	0.720	1.480	1.210	1.465	0.835
50	2.050	1.065	0.120	0.895	0.540	1.105	1.155	1.535	0.260	0.350
51	1.430	1.165	1.290	1.145	0.725	0.695	1.365	1.975	0.510	0.730
52	1.805	1.355	0.820	1.515	1.255	0.865	1.110	0.745	1.340	1.215
54	2.350	0.845	0.320	0.740	0.970	1.215	1.100	0.345	0.520	1.055
55	1.995	0.895	0.015	0.240	0.750	1.135	0.885	0.010	1.115	1.145
56	2.570	1.560	0.335	1.375	1.145	1.235	0.540	0.395	1.630	1.925
57	1.755	1.685	0.315	0.740	0.990	0.825	0.640	0.825	2.110	0.670
60	2.155	0.910	0.000	0.445	0.755	0.900	0.825	0.020	1.065	2.135
61	2.340	1.335	0.010	0.850	0.730	1.040	0.385	0.020	0.810	1.420
64	1.690	0.700	0.000	0.515	0.425	1.140	0.260	0.000	1.125	0.125
72	2.335	2.005	0.090	1.510	0.955	0.760	0.260	0.100	1.640	1.345
88	2.085	1.020	0.845	0.935	1.180	1.100	0.915	0.485	0.685	1.045
89	1.840	1.135	0.390	1.275	0.605	0.970	1.180	1.455	0.390	0.505
90	1.670	1.070	1.170	1.425	1.035	0.780	1.165	0.855	0.530	1.015
91	2.255	0.955	0.155	0.575	1.085	1.310	1.025	0.075	1.180	1.955

If a pair of raingages has a high positive correlation coefficient (close to 1), there is a strong positive relationship between the gages. Conversely, if the pair of gages has a high negative correlation coefficient (close to -1), there is a strong negative relationship between the gages. In this work, an attempt was made to select the gages that had the lowest absolute value of correlation coefficients (closest to zero) and select gages that had no apparent relationship to one another, consequently resulting in the gages that most accurately captured the spatial variability of the storms.

Case 4 used a "small" set of 3 raingages. Stemming from the work of Osborn et al. (1972), this sample size represented the minimum number of gages that should be used in order to accurately predict runoff. These gages were again selected on a random basis for each of 15 samples.

The final case, Case 5, used data from the small set of 3 raingages which were selected using the same minimization of correlation technique that was used to selected the gages in Case 3. The specific gages that were selected for Case 3 and Case 5 using the minimization of correlation procedure are shown in Table 4.2 below.

Table 4.2. Gages Selected Using Minimization of Correlation Procedure

Case No.	Sample Size	Gages with Minimum Correlation
3	3	38, 88, 57
5	9	38, 88, 57, 90, 44, 43, 60, 64, 51

4.3 Results and Analysis

The results of the simulations of the 5 different gage networks for each of the 2 storm events are summarized in Table 4.3. For each simulation, the modeled hydrograph was compared to the actual recorded hydrograph using the same metrics as discussed in the calibration and validation processes including percent error in peak discharge, peak timing error, and percent error in total runoff volume.

For the first storm event, storm V2, the control case produced peak discharge, peak timing, and total volume errors of 1.5%, 6 min, and 31.4% respectively. Case 2 produced average peak discharge, peak timing, and total volume errors of 31.4%, 6.8 min, and 29.4% respectively. Case 3 produced a peak discharge, peak timing, and total volume error of 13.8%, 12 min, and 36.5% respectively. Case 4 produced average peak discharge, peak timing, and total volume errors of 55.9%, 12 min, and 59.6% respectively. Case 5 produced a peak discharge, timing, and total volume error of 26.9%, 12 min, and 22.4% respectively.

With regard to peak discharge, the control case produced better results than the all of the other four cases. The next case which also closely fit the actual peak discharge of the storm event was Case 3, the medium number of gages that was selected using the minimization of correlation technique. It should also be noted that both of the gage samples selected using the minimization of correlation technique produced more accurate results than the randomly selected samples, and the randomly selected medium number of gages produced simulation results with an average of approximately 25% less error than that of the randomly selected small number of gages.

Table 4.3. Gage Reduction Results

Case No.	Absolute Peak Flow Error (%)				Absolute ΔPeak Timing (min)				Absolute Total Volume Error (%)			
	Mean	Max	Min	Std. Dev	Mean	Max	Min	Std. Dev	Mean	Max	Min	Std. Dev
Storm Event No. V2 - 8/04/2002												
1	1.5	-	-	-	6.0	-	-	-	31.4	-	-	-
2	31.4	49.2	-74.4	33.6	6.8	12.0	-24.0	10.0	29.4	75.5	-54.2	30.7
3	13.8	-	-	-	12.0	-	-	-	36.5	-	-	-
4	55.9	158.1	-90.8	70.0	12.0	30.0	-30.0	15.7	59.6	184.1	-83.3	71.8
5	26.9	-	-	-	12.0	-	-	-	22.4	-	-	-
Storm Event No. V3 - 7/31/2007												
1	1.6	-	-	-	12.0	-	-	-	31.2	-	-	-
2	51.6	108.0	-35.8	56.6	6.8	18.0	-6.0	6.8	54.2	136.5	-18.0	58.1
3	23.7	-	-	-	6.0	-	-	-	50.9	-	-	-
4	70.6	165.3	-100.0	75.9	6.0	24.0	-6.0	8.6	72.6	145.5	-100.0	78.5
5	16.6	-	-	-	12.0	-	-	-	29.0	-	-	-

Regarding peak timing for storm event V2, the control case again performed better than the other four samples, resulting in the lowest error. The simulations using the randomly selected medium number of gages resulted in a slight increase in error, but performed better than each of the remaining three samples, which all had the same error in peak timing.

With regard to total runoff volume for storm event V2, Case 5, the small number of gages selected using the minimization of correlation procedure, resulted in the lowest error. The control case and the randomly selected medium number of gages had slightly more error than Case 5, but had no significant difference among them. When comparing the two cases with randomly selected gages, the medium number of gages resulted in a 30% decrease in error over that of the small number of gages, as can be expected from increasing the number of gages used to provide inputs to the model.

Moving on to the second storm event, storm V3, the control case produced peak discharge, peak timing, and total volume errors of 1.6%, 12 min, and 31.2% respectively. Case 2 produced average peak discharge, peak timing, and total volume errors of 51.6%, 6.8 min, and 54.2% respectively. Case 3 produced peak discharge, timing, and total volume errors of 23.7%, 6 min, and 50.9% respectively. Case 4 produced average peak discharge, peak timing, and total volume errors of 70.6%, 6 min, and 72.6% respectively. Case 5 produced peak discharge, peak timing, and total volume errors of 16.6%, 12 min, and 29% respectively.

With regard to peak discharge for storm event V3, the control case using all of the 18 gages again resulted in the least amount of error. Overall, the samples selected

using the minimization of correlation method produced simulation results with a lower error than each of the randomly selected samples, and the randomly selected medium number of gages resulted in a 19% decrease in error from that of the randomly selected small number of gages.

Regarding peak timing for storm event V3, the medium number of gages selected using the minimization of correlation technique and the randomly selected small number of gages produced simulation results with the least amount of error. The randomly sampled medium number of gages produced simulation results with a slightly larger amount of error than these two cases, but was not a significant change. The control case and the small number of gages selected using the minimization of correlation approach resulted in the highest amount of error in peak timing among the five cases.

Regarding total runoff volume for the second storm event, the small number of gages selected using the minimization of correlation technique resulted in the least amount of error. The control case resulted in a slight increase in error from this case, but was not a significant change. Both of the samples selected using the minimization of correlation procedure resulted in a lower amount of error than their counterparts selected on a random basis. Also, the medium number of gages selected randomly resulted in an 18% decrease in error from that of the small number of gages selected randomly.

Overall, the control cases best simulated the peak discharge of the two storm events, which is what can be expected from using all of the available 18 raingages to provide information to the model. While this minimal amount of error might at first seem very appealing, when only half of these gages are used and are selected using the

minimization of correlation technique, the result is an average increase in error of only 17%. Furthermore, when looking at the error in peak discharge produced using the small number of three gages selected by the minimization of correlation technique, this error only increases by an additional 3%. This is small price to pay to be able to reduce the required gages by such a substantial amount.

It was found that the randomly selected medium number of gages produced better results in all categories (with the exception of peak timing for the second storm event) than those of the randomly selected small number of gages. Specifically, the error in peak discharge decreased by an average of 22%, and the total volume error decreased by an average of 25%. This also conformed to the initial expectations that by adding additional information to the system, there would be an increase in accuracy.

In general, the simulations using inputs from the raingages selected by the minimization of correlation technique produced results with less error than those using the randomly selected gages. This indicates that the minimization of correlation technique that was outlined in the previous section is a viable method for identifying gages that can be removed from a gage network. For the most part, when the number of gages providing inputs to the model was increased, the results got better. However, in some cases, the smallest number of gages produced results with the least amount of error. This indicates that sometimes a large gage network is not only undesirable because of its high cost, but that it also might be adding insignificant data to the system and can actually reduce a model's accuracy.

5. CONCLUSIONS AND FUTURE WORK

The timely and accurate forecasting of flash floods is a field of great importance, particularly to railroads in the western United States. These extreme hydrologic events cause millions of dollars in damages to railway infrastructure each year and can even lead to casualties among railroad personnel. The unique challenges that exist in the remote arid and semi-arid western U.S. require creative and innovative solutions to deal with this problem. Previous work suggests that to achieve reliable flash flood forecasting, one of the best options is to combine a physically-based, distributed-parameter hydrologic model with either radar estimates (if adequate coverage is available) or real-time raingage sensor measurements. To further add to the usefulness of the system, the resulting model predictions should be incorporated into a real-time decision support system that provides understandable estimates of flash flood potential to all users, even those who are not skilled in hydrology. When real-time sensor measurements are utilized, the selection of an appropriate gage density and the placement locations of these gages must take into consideration both the spatial variability of the storms as well as the economic limitations that exist.

In this work, a hydrologic model was developed that is capable of effectively describing the rainfall-runoff relationship of extreme, high intensity thunderstorms in arid and semi-arid regions. This model was calibrated and validated using precipitation and runoff data from ten summertime convective thunderstorms at the semi-arid Walnut Gulch Experimental Watershed located in southeastern Arizona. Also, a methodology is

proposed for reducing the amount of raingages required to provide acceptable inputs to the hydrologic model, and determining the most appropriate placement location for these gages. For two highly variable storm events used in the validation process, a control case in which a network of 18 raingages was used was compared to 4 scenarios that used a medium number of 9 gages and a small number of 3 gages, with gage locations being selected both randomly and using a minimization of correlation technique.

The results of the validation process show that the RHHMS hydrologic model is capable of reproducing peak discharge, peak timing, and total runoff volume to within an average of 22.1%, 12 min, and 32.8% respectively. Several improvements could be made that might have enhanced the performance of the model. One consideration is the use of a smaller grid cell size. Another potential improvement would be the incorporation of surveyed cross-sectional data. This would eliminate the need for the trapezoidal simplification of the channel geometry and in all likelihood lead to an increase in model accuracy.

The results of the gage reduction procedure show that a decrease in the amount of raingages used to drive a hydrologic model in this environment results in a disproportionally smaller decrease in model accuracy. Likewise, it was found that a reduction in gages will not always result in a decline in model accuracy. The results also indicate that choosing gages based on a minimization of correlation approach that seeks to select gages that with the lowest correlation of rainfall depths among storms (i.e. highest spatial variability) is a viable option over simply selecting these gages on a random basis.

There is ample potential for extending this research and furthering the development of a fully operational Railway Hydraulic Hazard Monitoring System. Like any model, there is always room for improvement, but the results acquired from the model as well as the lessons learned in its development will serve as a suitable starting point for additional investigation. One possible extension of the project would be to further test the model at another experimental watershed. Another extension of this project is the possibility of extending the modeling efforts of RHHMS to the more humid, eastern U.S. While this would surely change many of the key model components, including requiring the addition of a saturation-excess runoff mechanism and taking groundwater interaction into account, it would also allow for the utilization of precipitation data from radar estimates and possibly increase the warning time of the resulting model predictions, while decreasing the amount of gages that would be required to operate the model. Finally, the ultimate test of the model and an assessment as to the feasibility of RHHMS would involve a prototype of the system, implemented at a test watershed instrumented with real-time raingage and soil moisture sensors, and containing a railroad bridge or culvert crossing.

REFERENCES

American Meteorological Society (AMS), (1985), "Flash floods—a statement of concern by the American Meteorological Society", *Bulletin of the American Meteorological Society*, 66 (7), 858-859.

Anderson, M. G., and Burt, T. P., (1985), "Modelling strategies", *Hydrological forecasting*, John Wiley & Sons, New York, NY, 1-13.

Blanton, P., and Marcus, W. A., (2009), "Railroads, roads and lateral disconnection in the river landscapes of the continental United States." *Geomorphology*, 112 (3-4), 212-227.

Bras, R. (1990), "Hydrology: an introduction to hydrologic science", Reading, MA: Addison-Wesley, 643pp.

Burnash, R. J. C., Ferral, R. L., and McGuire, R. A., (1973), "A generalized streamflow simulation system—Conceptual modeling for digital computers", *Joint Federal–State River Forecast Center Tech. Rep.*, Department of Water Resources, State of California, and National Weather Service, 204 pp.

Devore, J. L., (2009), "Correlation", *Probability and statistics for engineering and the sciences*, 7th Ed., Brooks/Cole, Cengage Learning, Belmont, CA, NJ, 485-492.

Downer, C. W., Ogden, F. L., Martin, W., and Harmon, H. S., (2002), ''Theory, development, and applicability of the surface water hydrologic model CASC2D.'' *Hydrological Processes,* 16 (2), 255–275.

Downer, C. W., and Ogden, F. L., (2003), "Prediction of runoff and soil moistures at the watershed scale: Effects of model complexity and parameter assignment", *Water Resources Research*, 39 (3), 1045.

Downer, C. W., and Ogden, F. L., (2004), "GSSHA: Model to simulate diverse stream flow producing processes", *Journal of Hydrologic Engineering, ASCE,* 9 (3), 161-174.

Downer, C. W., and Ogden, F. L., (2006), "Gridded Surface Subsurface Hydrologic Analysis (GSSHA) user's manual, version 1.43 for Watershed Modeling System 6.1", System Wide Water Resources Program, Coastal and Hydraulics Laboratory, U.S. Army Corps of Engineers, Engineer Research and Development Center, ERDC/CHL SR-06-1, 207 pp.

Federal Railroad Administration (FRA), (2011), Federal Railroad Administration Office of Safety Analysis, available at: http://safetydata.fra.dot.gov/OfficeofSafety/default.aspx.

Gray, D. (1970), "Handbook on the principles of hydrology", National Research Council of Canada, Water Information Center Inc., Water Research Building, Manhasset Isle, Port Washington, NY.

Green, W., and Ampt, G. (1911), "Studies of soil physics, 1: Flow of air and water through soils", *Journal of Agricultural Sciences*, 4, 1-24.

Gupta, H., and Schaffner, M., (2006), "Development of a site-specific flash flood forecasting model for the western region", COMET Cooperative Project, University Corporation for Atmospheric Research, Boulder, Colorado.

Horton, R. E., (1933), "The role of infiltration in the hydrologic cycle", *Transactions – American Geophysical Union*, 14, 446-460.

Huff, W. E., Brumbelow, J. K., and Cahill, A., (2012), "Identifying railway hydraulic hazards", *Proc., 2012 AWRA Spring Specialty Conference*, AWRA, New Orleans, LA, March 26-28, 2012.

Julien, P., Saghafian, B., and Ogden, F. (1995), "Raster-based hydrologic modeling of spatially-varied surface runoff", *Water Resources Bulletin,* 31 (3), 523-536.

Knapp, H., Durgunoglu, A., and Ortel, T. (1991), "A review of rainfall-runoff modeling for stormwater management", *Illinois State Water Survey*, *Hydrology Division*, Champaign, Illinois.

Kohler, M. A., and Linsley, R. K., (1951), "Predicting runoff from storm rainfall", *Research Paper*, 43, U.S. Weather Bureau.

Kuichling, E., (1889), "The relationship between the rainfall and discharge of sewers in populous districts", *Transactions of the American Society of Civil Engineers*, Vol. 20.

Lloyd, J. W., (1986), "A review of aridity and groundwater", *Hydrological Processes*, 1(1), 63-78.

McIntyre, D.S., (1958), "Permeability measurements of soil crusts formed by raindrop impact", *Soil Science*, 85 (4), 185-189.

Mein, R. G., and Larson, C. L., (1973), "Modeling infiltration during a steady rain", *Water Resources Research*, 9 (2), 384-394.

Multi-Resolution Land Characteristics Consortium (MRLC), (2006), National Land Cover Database 2006, available at: http://www.mrlc.gov/nlcd06_data.php.

National Oceanic and Atmospheric Administration (NOAA), (2012), National Climatic Data Center, available at: http://www.ncdc.noaa.gov/cdo-web/.

National Resources Conservation Service (NRCS), (1986), "Urban hydrology for small watersheds", *Technical Release 55*, *US Department of Agriculture*, Washington, D.C.

National Weather Service (NWS), (2002), "Advanced hydrologic prediction services—concept of services and operations". *Report, US Department of Commerce – NOAA – NWS*, USA.

Neary, D. G., Ryan, K. C., DeBano, L. F., (2005), "Wildland fire in ecosystems: effects of fire on soils and water", General Technical Report RMRS-GTR-42-vol.4, Ogden, UT: U.S. Department of Agriculture, Forest Service, Rocky Mountain Research Station, 250 pp.

Ogden, F., Sharif, H., Senerath, S., Smith, J., Baeck, M., and Richardson, J. (2000), "Hydrologic analysis of the Fort Collins, Colorado, flash flood of 1997", *Journal of Hydrology*, 228 (1-2), 82-100.

Osborn, H. B., Lane, L. J., and Hundley, J. F., (1972), "Optimum gaging of thunderstorm rainfall in southeastern Arizona", *Water Resources Research*, 8 (1), 259-265.

Osborn, H. B. and Renard, K. G., (1970), "Thunderstorm runoff on the Walnut Gulch experimental watershed, Arizona, U.S.A.", *Symposium on the results of research on representative and experimental basins*, IASH-Unesco, Wellington, N.Z., December, 1970.

Peschel, J., Brumbelow, J. K., and Cahill, A., (2010), "A real-time interface for railway hydraulic hazard forecasting", *World Environmental & Water Resources Congress*, *Bearing Knowledge for Sustainability*, Palm Springs, CA, May 22-26, 2011.

Rawls, W. J., Brakensiek, D. L. and Miller, N., (1983), "Green-Ampt infiltration parameters from soils data", *Journal of Hydraulic Engineering*, ASCE, 109 (1): 62-70.

Renard, K. G., Nichols, M. H., Woolhiser, D. A., Osborn, H. B., (2008), "A brief background on the U.S. Department of Agriculture Agricultural Research Service Walnut Gulch Experimental Watershed", *Water Resources Research*, (44) W05S02, doi:10.1029/2006WR005691.

Rojas, R., Julien, P., and Johnson, B. (2003), "A two-dimensional rainfall-runoff and sediment model", Colorado State University, Ft. Collins, CO, 140pp.

Senarath, S. U. S., Ogden, F. L., Downer, C. W., and Sharif, H. O., (2000), "On the calibration and verification of two-dimensional, distributed, Hortonian, continuous watershed models", *Water Resources Research,* (36) 6, 1495–1510.

Sharif, H. O., Almoutaz, A. H., Sazzad, B. S., Xie, H., and Zeitler, J. (2010), "Hydrologic modeling of an extreme flood in the Guadalupe River in Texas", *Journal of the American Water Resources Association*, 46 (5), 881-891.

Sherman, L. K., (1932), "Streamflow from rainfall by the unit graph method", *Engineering News Record*, 108, 501-505.

Sittner, W., Schauss, C., and Monro, J., (1969), "Continuous hydrograph synthesis with an API-type hydrologic model", *Water Resources Research*, 5 (5), 1007-1022.

United States Department of Agriculture Agricultural Research Service (USDA-ARS), (2012), Online data access, Southwest Watershed Research Center, available at: http://www.tucson.ars.ag.gov/dap/.

United States Department of Agriculture (USDA), (2011), National Resources Conservation Service Soil Data Mart, available at: http://soildatamart.nrcs.usda.gov/.

United States Department of Agriculture (USDA), (2003), "Walnut Gulch experimental watershed", Southwest Watershed Research Center, Tucson, Arizona, 44 pp.

United States Geological Service (USGS), (2011a), National Elevation Dataset, available at: http://ned.usgs.gov/.

United States Geological Service (USGS), (2011b), National Hydrography Dataset, available at: http://nhd.usgs.gov/.

Weather Underground, (2011), "Radar frequently asked questions", available at: http://www.wunderground.com/radar/help.asp.

Wechsler, S. P., (2007), "Uncertainties associated with digital elevation models for hydrologic applications: A review, *Hydrology and Earth Systems Sciences*, 11(4), 1481-1500.

Woolhiser, D., Smith, R., and Goodrich, D., (1990), "KINEROS: A kinematic runoff and erosion model documentation and user manual", *USDA-Agricultural Research Service Publication, ARS-77*, 130 pp.

Wurbs, R., and James, W., (2002), "Modeling watershed hydrology", *Water resources engineering*, Pretence-Hall, Upper Saddle River, NJ, 462-533.

Yatheendradas, S., (2007), "Flash flood forecasting for the semi-arid southwestern United States", dissertation, presented to the University of Arizona, at Tucson, AZ, in partial fulfillment of the requirements for the degree of Doctor of Philosophy.

Yatheendradas, S., Wagener, T., Gupta, H., Unkrich, C., Goodrich, D., Schaffner, M., and Stewart, A., (2008), "Understanding uncertainty in distributed flash flood forecasting for semiarid regions", *Water Resources Research*, 44 (5), W05S19, 17 pp.